ANL-GIF-SO-2018-2
SFR-SO-2018-010

BOP-301 and BOP-302R: Test Definitions and Analyses

Nuclear Science and Engineering Division

About Argonne National Laboratory
Argonne is a U.S. Department of Energy laboratory managed by UChicago Argonne, LLC under contract DE-AC02-06CH11357. The Laboratory's main facility is outside Chicago, at 9700 South Cass Avenue, Argonne, Illinois 60439. For information about Argonne
and its pioneering science and technology programs, see www.anl.gov.

ANL-GIF-SO-2018-2
SFR-SO-2018-010

BOP-301 and BOP-302R: Test Definitions and Analyses

prepared by
T. Sumner, G. Zhang, and T. H. Fanning
Nuclear Science and Engineering Division, Argonne National Laboratory

December 31, 2018

ABSTRACT

Following the conclusion of the International Atomic Energy Agency (IAEA) coordinated research project (CRP) on analysis of two EBR-II tests, Argonne has continued its EBR-II analysis with additional tests from the Shutdown Heat Removal Test (SHRT) series. The tests selected for this follow-up analysis are BOP-301 and BOP-302R, two unprotected loss of heat of sink tests in which the intermediate sodium pump tripped without scramming the control rods or tripping the primary pumps.

The IAEA CRP focused on the SHRT-17 and SHRT-45R tests, the most severe protected and unprotected loss of flow tests performed during the SHRT series. With the primary pumps tripping, flow rates decreased to levels where flowmeter uncertainty was very high. Accurately capturing the progressions of the two tests despite this uncertainty was one of the key modeling and simulation challenges during the CRP.

BOP-301 and BOP-302R were selected because the primary sodium pumps did not trip for those tests. Primary flow rate measurements are known with greater certainty. Power and temperature discrepancies can be explored without concern that flow predictions match test measurements but not the actual flow rates from the tests. These two tests were performed during the same test window as SHRT-45R and had the same core load configuration. Therefore, core models created for analysis of SHRT-45R were easily adapted for analysis of BOP-301 and BOP-302R.

Another reason for analyzing BOP-301 and BOP-302R is to analyze tests in which the core inlet temperature changed significantly, which did not occur during the loss of flow tests. The transient progression of the unprotected SHRT-45R test was driven by a decreasing core flow rate while the core inlet temperature remained relatively constant. For the BOP tests, the transient progression was driven by an increasing core inlet temperature while the core flow rate was stable.

This report defines the BOP-301 and BOP-302R tests and provides a selection of measured test data. Initial predictions from SAS4A/SASSYS-1 simulations of these tests are then presented. Following these simulations, additional analysis was performed with the Dakota uncertainty quantification and optimization toolkit to determine which parameters have the greater impact on the transient results and the optimal values of the most important parameters.

TABLE OF CONTENTS

Abstract iii
Table of Contents v
Table of Figures vi
Table of Tables vii
Acronyms viii
1 Introduction 1
2 Test Definitions 2
2.1 BOP-301 2
2.2 BOP-302R 5
3 Measured Test Data 9
3.1 BOP-301 9
3.2 BOP-302R 13
4 SAS4A/SASSYS-1 Model 18
5 Initial SAS4A/SASSYS-1 Predictions 22
5.1 BOP-301 22
5.2 BOP-302R 25
6 Uncertainty Quantification and Optimization 28
6.1 Dakota and SAS4A/SASSYS-1 Coupling 28
6.2 Sensitivity Analysis of the EBR-II BOP Simulation 30
6.3 Optimization of EBR-II BOP Simulation Results 34
7 Summary 40
Electronic Appendix A 42
Electronic Appendix B 43
References 44

TABLE OF FIGURES

Figure 2.1. BOP-301 Intermediate Side Flow Rate, Low Range 3
Figure 2.2. BOP-301 IHX Intermediate Side Inlet Temperature 3
Figure 2.3. BOP-302R Intermediate Side Flow Rate, Low Range 6
Figure 2.4. BOP-302R IHX Intermediate Side Inlet Temperature 6
Figure 3.1. BOP-301 Normalized Power 9
Figure 3.2. BOP-301 Core Inlet Temperature Measurements 10
Figure 3.3. BOP-301 Z-Pipe Inlet Temperature Measurement 11
Figure 3.4. BOP-301 IHX Primary-Side Temperature Measurements 12
Figure 3.5. BOP-301 Primary Flow Measurements 13
Figure 3.6. BOP-302R Normalized Power 14
Figure 3.7. BOP-302R Core Inlet Temperature Measurements 15
Figure 3.8. BOP-302R Z-Pipe Inlet Temperature Measurement 15
Figure 3.9. BOP-302R IHX Primary-Side Temperature Measurements 16
Figure 3.10. BOP-302R Primary Flow Measurements 17
Figure 4.1. SAS4A/SASSYS-1 Core Channel Geometry 18
Figure 4.2. BOP-301 and BOP-302R SAS4A/SASSYS-1 Channels 19
Figure 4.3. EBR-II Primary System PRIMAR-4 Model 20
Figure 5.1. BOP-301 Core and Z-Pipe Inlet Temperatures 22
Figure 5.2. BOP-301 Reactivity Feedbacks 23
Figure 5.3. BOP-301 Total Power 24
Figure 5.4. BOP-302R Core and Z-Pipe Inlet Temperatures 26
Figure 5.5. BOP-302R Reactivity Feedbacks 26
Figure 5.6. BOP-302R Total Power 27
Figure 6.1. Dakota and SAS4A/SASSYS-1 Coupling Scheme 29
Figure 6.2. Examples of Monte Carlo and Latin Hypercube Sampling Techniques 30
Figure 6.3. BOP-301 Core Inlet and Z-Pipe Inlet Temperatures – Original (Upper) vs. Optimized (Lower) models 36
Figure 6.4. BOP-302R Core Inlet and Z-Pipe Inlet Temperatures – Original (Upper) vs. Optimized (Lower) models 37
Figure 6.5. BOP-301 Total Power 38
Figure 6.6. BOP-302R Total Power 38

TABLE OF TABLES

Table 2.1. BOP-301 Initial Conditions 2
Table 2.2. BOP-301 Intermediate Side Flow Rate 4
Table 2.3. BOP-301 IHX Intermediate Side Inlet Temperature 4
Table 2.4. BOP-301 Normalized Primary Pump Conditions 5
Table 2.5. BOP-302R Initial Conditions 5
Table 2.6. BOP-302R Intermediate Side Flow Rate 7
Table 2.7. BOP-302R IHX Intermediate Side Inlet Temperature 7
Table 2.8. BOP-302R Normalized Primary Pump Conditions 8
Table 6.1. Impact of Uncertain Variables on SAS4A/SASSYS-1 Predictions 33
Table 6.2. Optimized SAS4A/SASSYS-1 Inputs Parameters 39

ACRONYMS

BOP – Balance of Plant
CRDL – Control Rod Driveline
CRP – Coordinated Research Project
CV – Compressible Volume
EBR-II – Experimental Breeder Reactor II
EM – Electromagnetic
IAEA – International Atomic Energy Agency
IHX – Intermediate Heat Exchanger
SHRT – Shutdown Heat Removal Test

1 Introduction

The International Atomic Energy Agency (IAEA) coordinated research project (CRP), "Benchmark Analyses of an EBR-II Shutdown Heat Removal Test", which concluded in 2016, focused on the SHRT-17 and SHRT-45R tests. [1,2] SHRT-17 and SHRT-45R were the most severe protected and unprotected loss of flow tests from the EBR-II Shutdown Heat Removal Test (SHRT) series. Argonne's analysis of SHRT-17 and SHRT-45R was performed with the fast reactor safety analysis code SAS4A/SASSYS-1. [3] While modeling and simulation of the SHRT tests concluded in 2016, Argonne has continued its EBR-II analysis with additional tests from the Shutdown Heat Removal Test (SHRT) series.

The first tests selected for this follow-up analysis are BOP-301 and BOP-302R, two unprotected loss of heat of sink tests in which the intermediate sodium pump tripped without scramming the control rods or tripping the primary pumps. The BOP, or balance of plant, tests were a series of tests performed during the SHRT program to investigate transients in which the primary sodium pumps did not trip. In different sets of BOP tests, the insertion depth of a single control rod or the head generated by the intermediate sodium electromagnetic (EM) pump was oscillated at various frequencies and initial power levels. The fourth SHRT testing window included BOP-301 and BOP-302R, two loss of heat of sink tests where the intermediate sodium pump tripped without a control rod scram or primary pump trip.

The BOP-301 and BOP-302R tests are attractive tests for follow-up analysis for several reasons. First, unlike SHRT-17 and SHRT-45R, the primary pumps did not trip, so 100% primary sodium flow was maintained. While the predicted SAS4A/SASSYS-1 flow rates for the two SHRT loss of flow tests agree well with the measured data, primary flow rates decreased to levels where the flow meter uncertainty was very high. Matching the measured flow rates could therefore cause discrepancies elsewhere in the model. Accurately capturing the progressions of the two tests despite this uncertainty was one of the key modeling and simulation challenges during the CRP. By analyzing tests where the primary pumps did not trip, the problem of large uncertainty in the flow rate measurements is eliminated.

The second reason for analyzing the two BOP tests is that they were performed during the same testing window as SHRT-45R and therefore had the same core load configuration. Neutronics calculations have already been performed for SHRT-45R for the IAEA benchmark, so the same core model that was used to analyze that test is valid for analyzing the two BOP tests. The third reason for analyzing BOP-301 and BOP-302R is that the core inlet temperature increases during these tests. During SHRT-45R, the core inlet temperature was relatively flat throughout the entire test. Reactivity feedbacks were induced solely by the decreasing flow rate. For the BOP tests, the model can be assessed under the reverse scenario where the flow rate is unchanged but the core inlet temperature changes significantly.

Section 2 of this report defines the tests and Section 3 provides the measured test data. The test definitions provided in this report are supplemented by the EBR-II reactor core and heat transport system geometric descriptions provided in the original SHRT-17 and SHRT-45R benchmark specification [4, 5]. The SAS4A/SASSYS-1 model used for analyzing these tests is described in Section 4. And Section 5 provides the results of the SAS4A/SASSYS-1 simulations of the BOP-301 and BOP-302R tests. Finally, Section 6 presents the results of analysis performed with the Dakota uncertainty quantification and optimization toolkit.

2 Test Definitions

BOP-301 and BOP-302R were similar tests. Both were initiated by an intermediate pump trip. The main difference between the two tests was that BOP-301 was initiated at 50% power while BOP-302R was initiated at 100% power. Initial conditions and transient boundary conditions for benchmark analysis of the two tests are defined below. Additional information on the EBR-II system is provided in the original EBR-II benchmark specification [4], which presents the geometry of the reactor core, various core subassemblies, and primary heat transport system. Subassembly compositions are provided in the SHRT-45R neutronics benchmark specification [5]. The same core configuration was used for SHRT-45R and the two BOP tests.

2.1 BOP-301

Table 2.1 defines the initial conditions for BOP-301. The test began when the intermediate sodium pump tripped. With limited heat rejection through the intermediate heat exchangers, the core inlet temperature gradually increased. The resulting negative reactivity feedback caused the power level to decrease nearly to zero without the control rods scramming.

Table 2.1. BOP-301 Initial Conditions

Parameter	Initial Value
Power	31.98 MW
Inner Core Mass Flow Rate	392.9 kg/s
Outer Core Mass Flow Rate	75.8 kg/s
Core Bypass Mass Flow Rate	3.91 kg/s
Intermediate Mass Flow Rate	202.2 kg/s
Core Inlet Temperature	616.9 K
Auxiliary EM Pump Current	9455.8 Amps

The IHX intermediate side inlet flow rate and temperature for BOP-301 are illustrated in Figures 2.1 and 2.2, respectively, and that data is tabulated in Tables 2.2 and 2.3. While the loss of flow tests were analyzed for 15 minutes, the BOP tests were run for more than 75 minutes. Reactor conditions, however, did not change significantly during the final 25 minutes, so the tests are defined for 50 minutes, or 3,000 seconds.

The primary sodium pump speeds and auxiliary EM pump current all remain relatively stable the test. Table 2.4 lists those values at various times during the test.

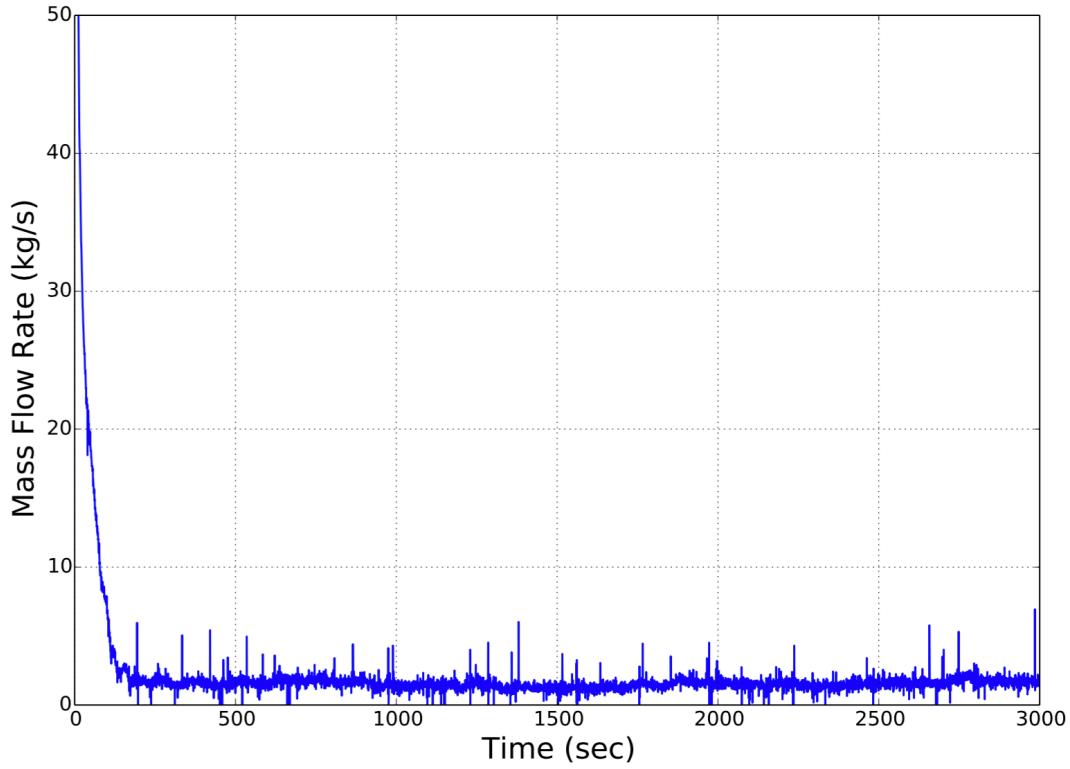

Figure 2.1. BOP-301 Intermediate Side Flow Rate, Low Range

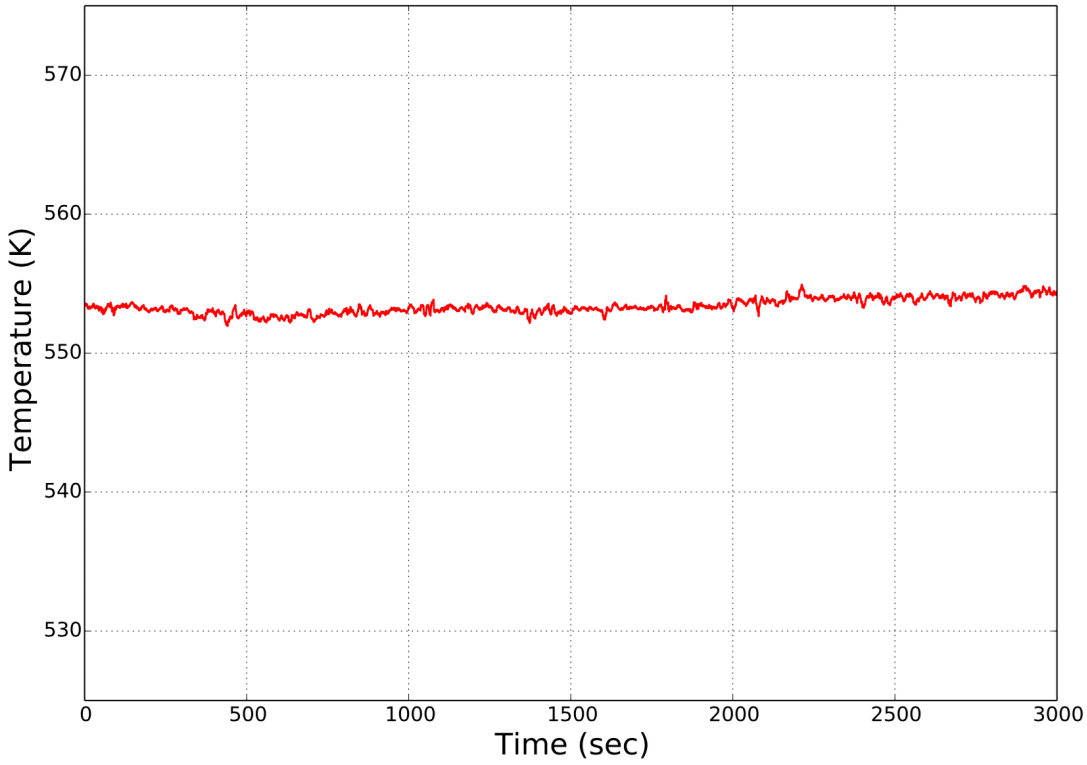

Figure 2.2. BOP-301 IHX Intermediate Side Inlet Temperature

Table 2.2. BOP-301 Intermediate Side Flow Rate

Time (s)	Flow Rate (kg/s)
0.0	202.228
0.5	192.526
1.5	142.550
4.5	93.576
9.5	55.282
20.1	33.686
53.5	17.384
98.5	7.430
148.5	2.484
198.5	2.065
248.5	1.780
498.5	1.372
998.5	1.741
1498.5	1.277
1998.5	1.026
2498.5	1.607
2998.5	1.886
3498.5	1.758
3998.5	1.584
4500.0	1.970

Table 2.3. BOP-301 IHX Intermediate Side Inlet Temperature

Time (s)	Temperature (K)
0.0	553.437
51.0	553.239
428.5	552.862
558.5	552.318
676.5	552.670
988.5	553.043
1378.5	552.927
1618.5	553.119
2008.5	553.394
2658.5	554.021
3098.5	554.416
3498.5	553.347
4003.5	551.626
4500.0	549.622

Table 2.4. BOP-301 Normalized Primary Pump Conditions

Time (s)	Auxiliary EM Pump Current	Pump #1 Speed	Pump #2 Speed
0.0	0.999	1.001	1.001
503.5	1.000	1.000	1.001
998.5	1.001	1.001	1.001
1498.5	1.003	1.000	1.000
1998.5	1.005	1.000	1.000
2498.5	1.006	1.000	1.000
2998.5	1.004	1.000	0.999
3498.5	1.006	1.000	1.000
3998.5	1.006	1.000	1.000
4498.5	1.004	1.000	1.000

BOP-301 was performed near the beginning of Run 138B. Prior to Run 138B, the reactor was shut down to reload the core. The exact power history during Run 138B is unknown. However, it is assumed that the reactor was operated at an average power of 29.86 MW for 8.45 hours, and then the total reactor power was ramped up from zero power to 30.98 MW over 7.0 hours. The reactor remained at this power level until the test started 9.2 minutes later.

2.2 BOP-302R

Table 2.5 defines the initial conditions for BOP-302R. The conditions for BOP-302R were very similar to the conditions for BOP-301, except that BOP-302R was initiated at a higher power level and intermediate sodium flow rate.

Table 2.5. BOP-302R Initial Conditions

Parameter	Initial Value
Power	59.89 MW
Inner Core Mass Flow Rate	391.4 kg/s
Outer Core Mass Flow Rate	75.5 kg/s
Core Bypass Mass Flow Rate	3.89 kg/s
Intermediate Mass Flow Rate	307.2 kg/s
Core Inlet Temperature	616.4 K
Auxiliary EM Pump Current	9316.7 Amps

The IHX intermediate side inlet flow rate and temperature for BOP-302R are illustrated in Figures 2.3 and 2.4, respectively, and that data is tabulated in Tables 2.6 and 2.7. As with BOP-301, BOP-302R is defined for 50 minutes, or 3,000 seconds. Table 2.8 lists the normalized primary pumps speed and current during BOP-302R.

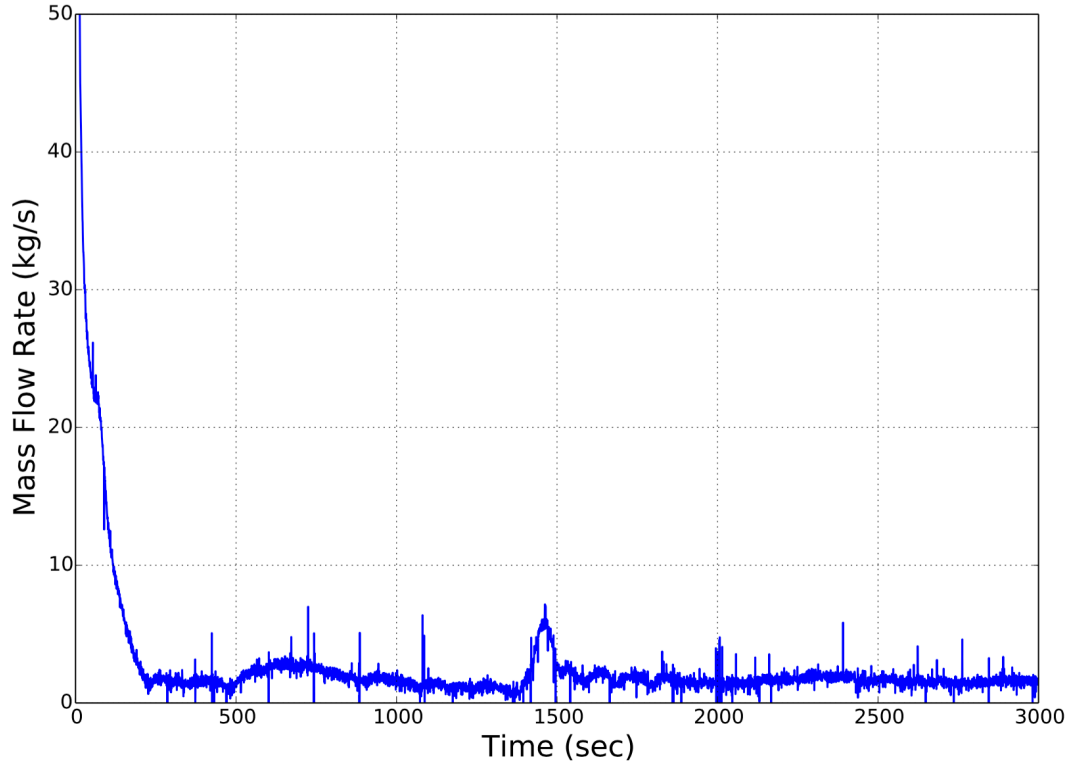

Figure 2.3. BOP-302R Intermediate Side Flow Rate, Low Range

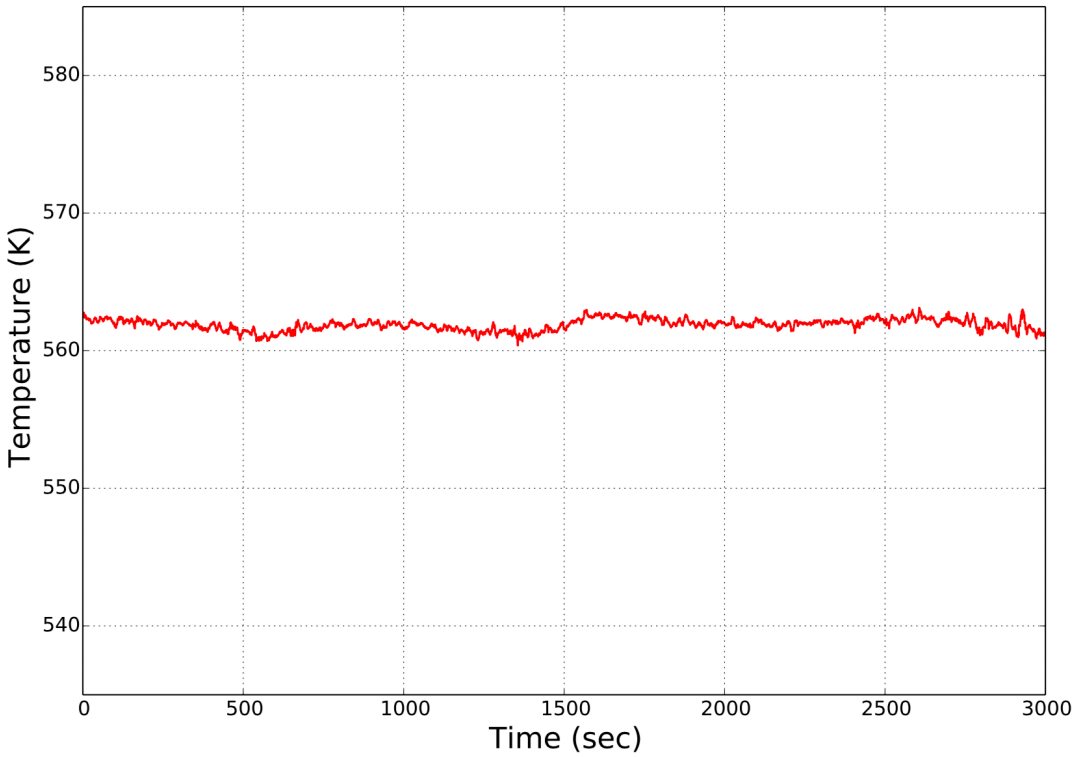

Figure 2.4. BOP-302R IHX Intermediate Side Inlet Temperature

Table 2.6. BOP-302R Intermediate Side Flow Rate

Time (s)	Flow Rate (kg/s)
0.0	307.162
0.5	292.351
1.5	191.518
4.5	108.019
9.5	61.321
20.0	37.168
53.5	24.274
98.5	13.639
148.5	6.478
198.5	2.454
248.5	1.813
498.5	1.312
998.5	1.830
1498.5	2.358
1998.5	1.425
2498.5	1.700
2998.5	1.588
3498.5	1.807
3998.5	1.549
4500.0	1.835

Table 2.7. BOP-302R IHX Intermediate Side Inlet Temperature

Time (s)	Temperature (K)
0.0	562.391
51.0	562.114
428.5	561.765
558.5	561.041
676.5	561.667
988.5	561.928
1373.5	561.273
1598.5	562.708
1998.5	562.004
2648.5	562.344
2998.5	561.281
3498.5	559.591
3999.0	557.775
4493.5	556.661

Table 2.8. BOP-302R Normalized Primary Pump Conditions

Time (s)	Auxiliary EM Pump Current	Pump #1 Speed	Pump #2 Speed
0.0	1.001	1.000	1.000
503.5	1.011	1.000	1.000
998.5	1.011	1.000	1.000
1498.5	1.018	0.999	0.999
1998.5	1.019	1.000	1.000
2498.5	1.019	1.000	1.000
2998.5	1.020	1.000	1.000
3498.5	1.024	1.000	1.000
3998.5	1.020	1.000	0.999
4498.5	1.022	1.001	1.001

BOP-302R was performed near the end of Run 138B. The exact power history during Run 138B is unknown. However, it is assumed that the reactor was operated at an average power of 31.31 MW for 122.6 hours, and then reactor power was ramped up from zero power to 59.89 MW over 7.1 hours. The reactor remained at this power level until the test started 8.6 minutes later.

3 Measured Test Data

EBR-II was heavily instrumented throughout its primary and intermediate systems. A set of measurements has previously been selected for comparison against simulation results for the SHRT-17 and SHRT-45R benchmarks [2]. These same measurements have been collected for BOP-301 and BOP-302R and are illustrated in figures below. Because measurements were recorded twice per second and data is presented for 3,000 seconds, tabulated data is not presented in this report. That data is available in Electronic Appendices A and B.

3.1 BOP-301

The normalized fission power was measured during each of the SHRT and BOP tests. During steady-state conditions, total power can be determined with flow and temperature measurements. But total power cannot be accurately measured during a transient. To provide data for comparison against simulation results, the total transient power was calculated. The assumed pre-transient power history provided in Section 2.1 was used to determine the amount of fission power and decay heat at the start of the test. Then, the transient decay heat was calculated based on the measured fission power. The resulting normalized total, fission, and decay heat power levels are shown in Figure 3.1.

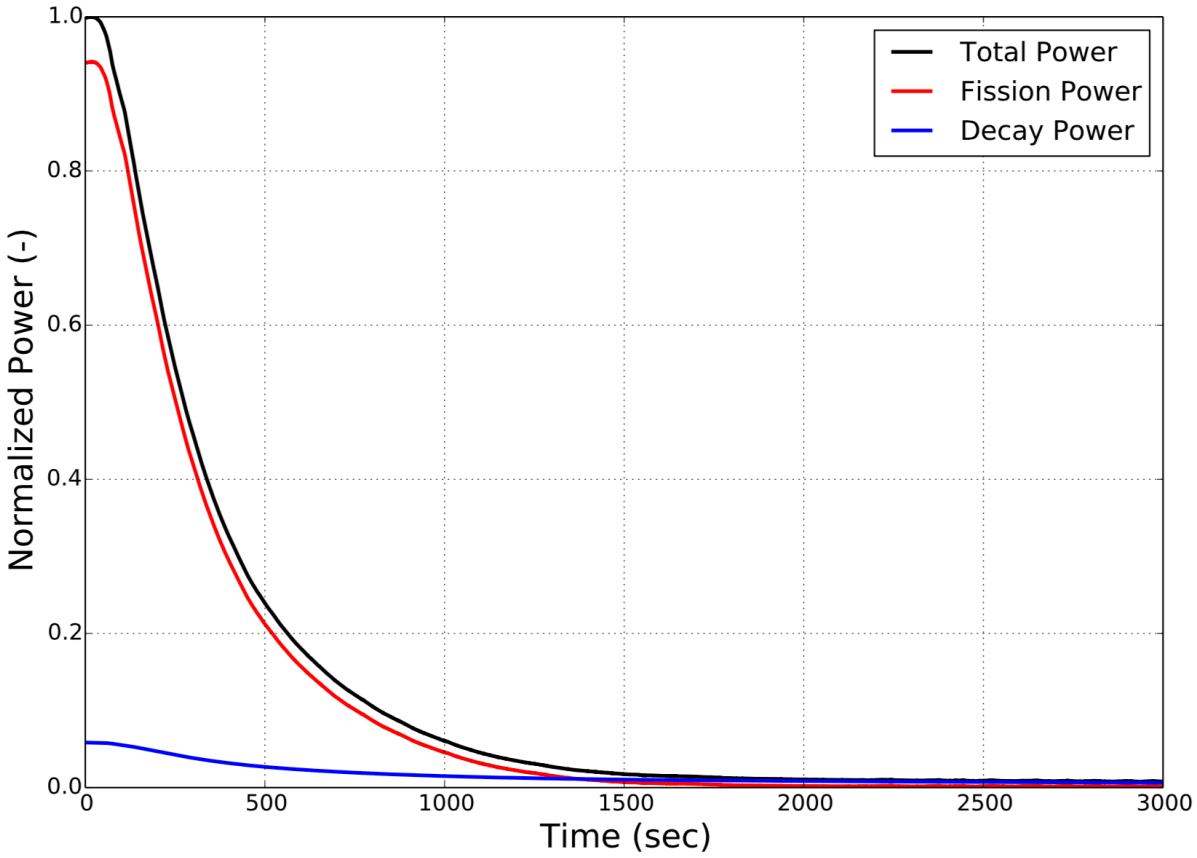

Figure 3.1. BOP-301 Normalized Power

A variety of thermocouples were installed to measure the core inlet and outlet temperatures. Figure 3.2 illustrates the high- and low-pressure inlet plena temperatures. Figure 3.3 illustrates the temperature of sodium at the Z-Pipe inlet. Temperatures were also recorded at various elevations directly above a blanket subassembly within the outlet plenum. However, systems codes like SAS4A/SASSYS-1 cannot accurately capture the complicated temperature distributions in the outlet plenum with 0-dimensional volumes, so those temperatures are not included in this report.

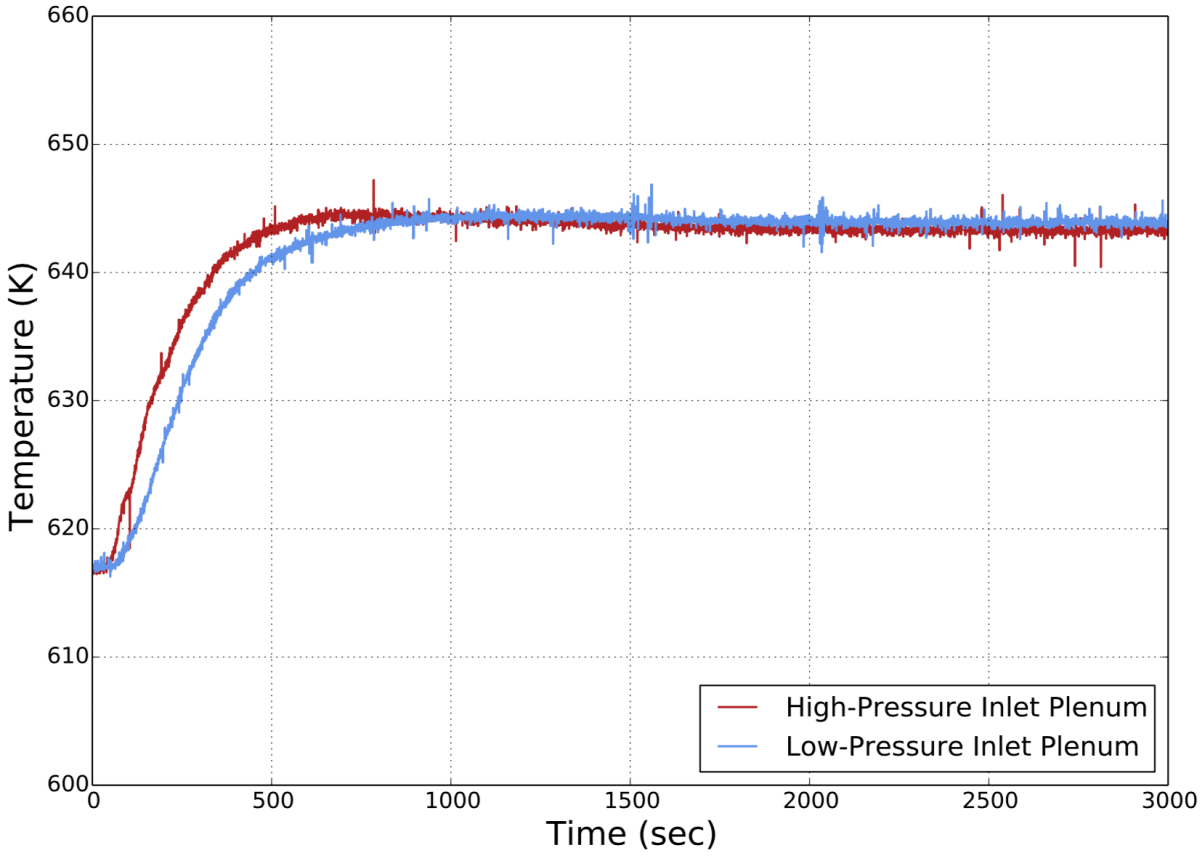

Figure 3.2. BOP-301 Core Inlet Temperature Measurements

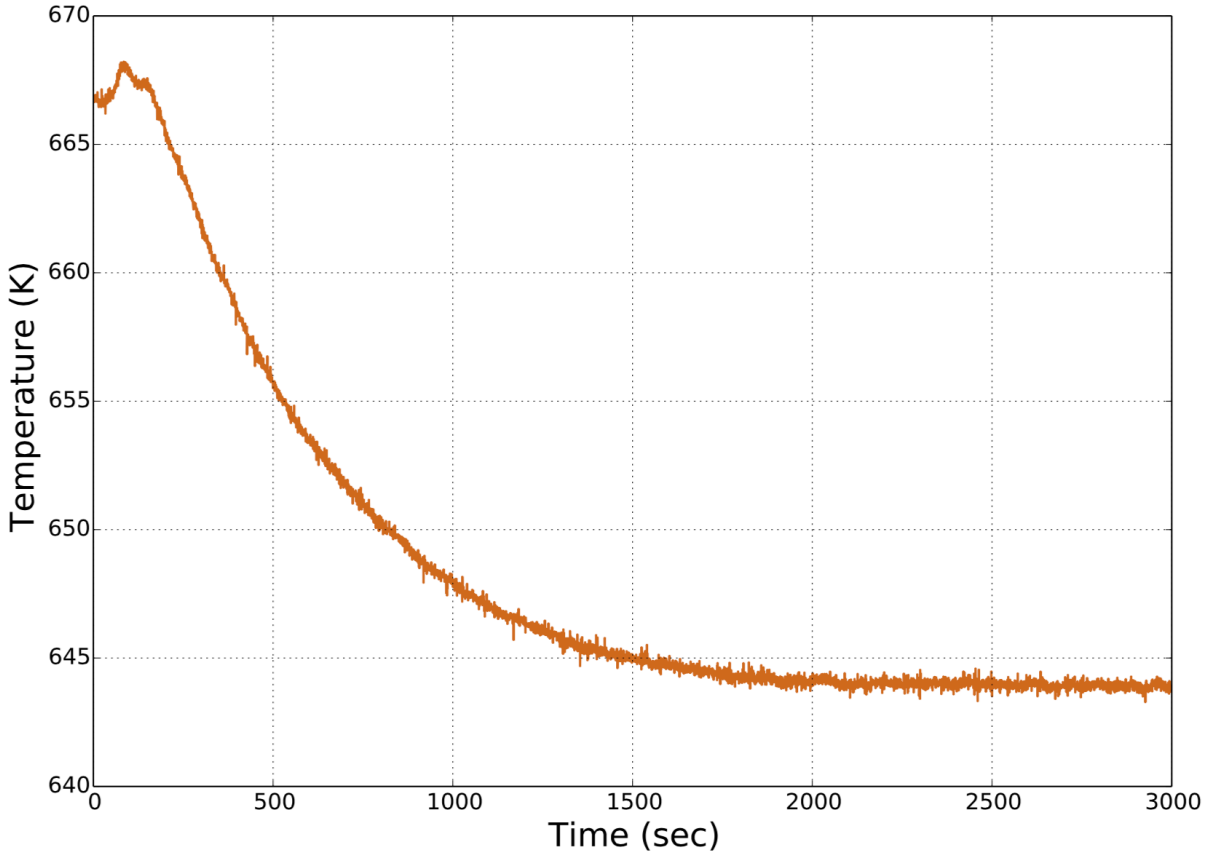

Figure 3.3. BOP-301 Z-Pipe Inlet Temperature Measurement

IHX primary-side temperatures are illustrated in Figure 3.4. Caution should be used when comparing the results of systems codes against these measurements. The inlet and outlet temperature measurements both appear to be heavily affected by their location. The inlet thermocouple was located behind two impact baffle plates along one of the IHX tubes. The temperature in that location likely did not represent average Z-Pipe outlet temperature, as thermal stratification, heat transfer with the IHX tubes, and complex flow patterns around the impact baffle plates produced a lower than expected temperature measurement.

The outlet thermocouples were located outside the IHX where sodium temperatures were not representative of the average IHX outlet temperature. Temperatures measured at the bottom orifice plate, which was inside the IHX approximately one foot above the outlet, were significantly different from the measured outlet temperatures and were much more similar to the inlet temperature measurements following the decrease of heat rejection through the IHX.

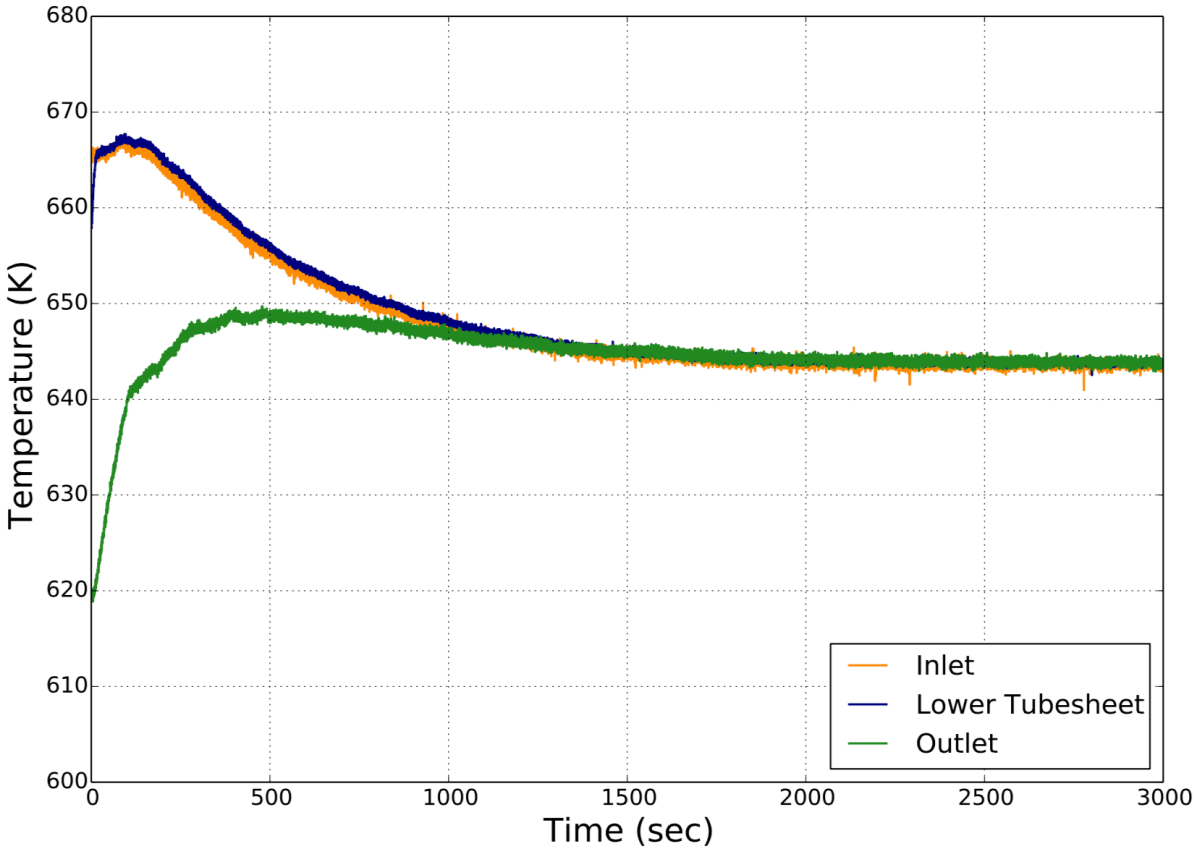

Figure 3.4. BOP-301 IHX Primary-Side Temperature Measurements

Although the primary pump speeds were maintained at 100% during the test, temperature changes throughout the primary system produced small flow rate changes. Figure 3.5 illustrates the flow rates that were measured in the high- and low-pressure piping following Pump #2. Although ten flowmeters were originally installed in the primary system, the flowmeters in the piping following Pump #1 had failed prior to the SHRT testing program.

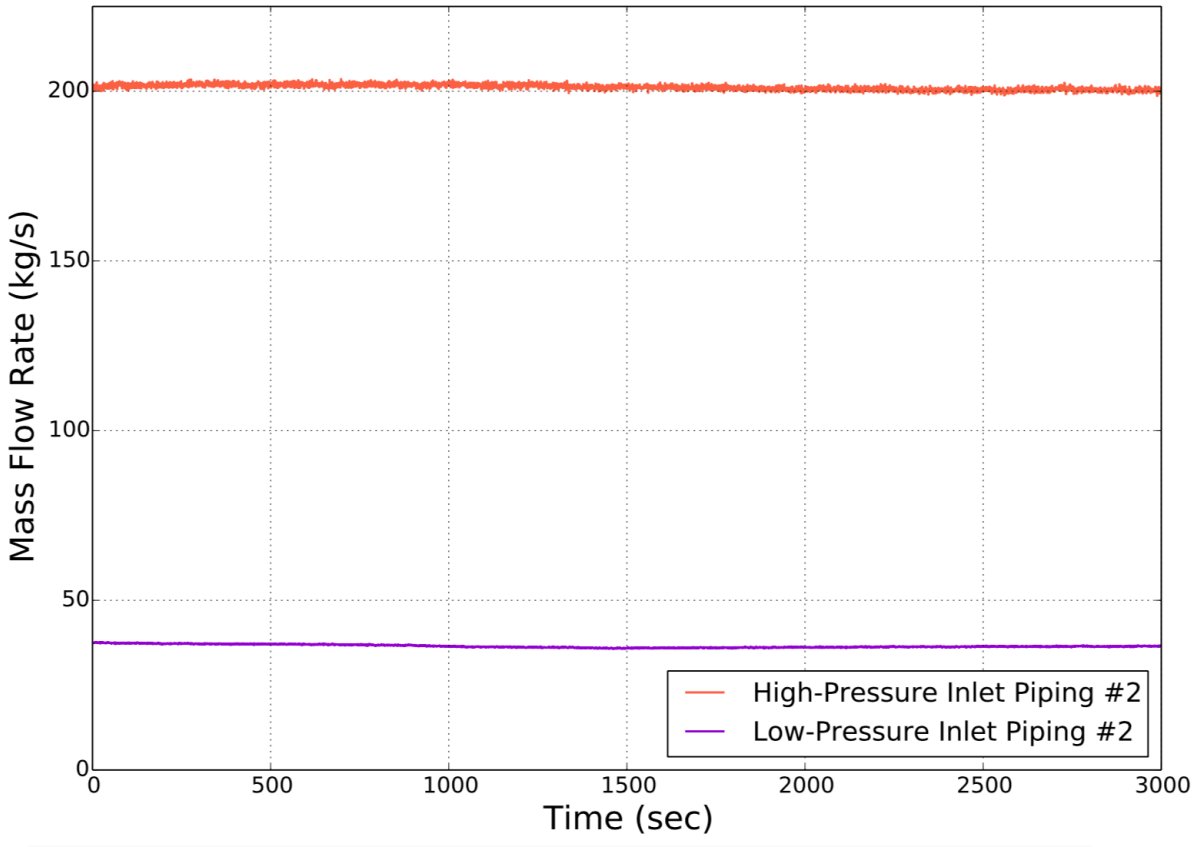

Figure 3.5. BOP-301 Primary Flow Measurements

3.2 BOP-302R

As with BOP-301, the assumed pre-transient power history provided in Section 2.2 was used to determine the amount of fission power and decay heat at the start of the test. Then, the transient decay heat was calculated based on the measured fission power. The resulting normalized total, fission, and decay heat power levels are shown in Figure 3.6.

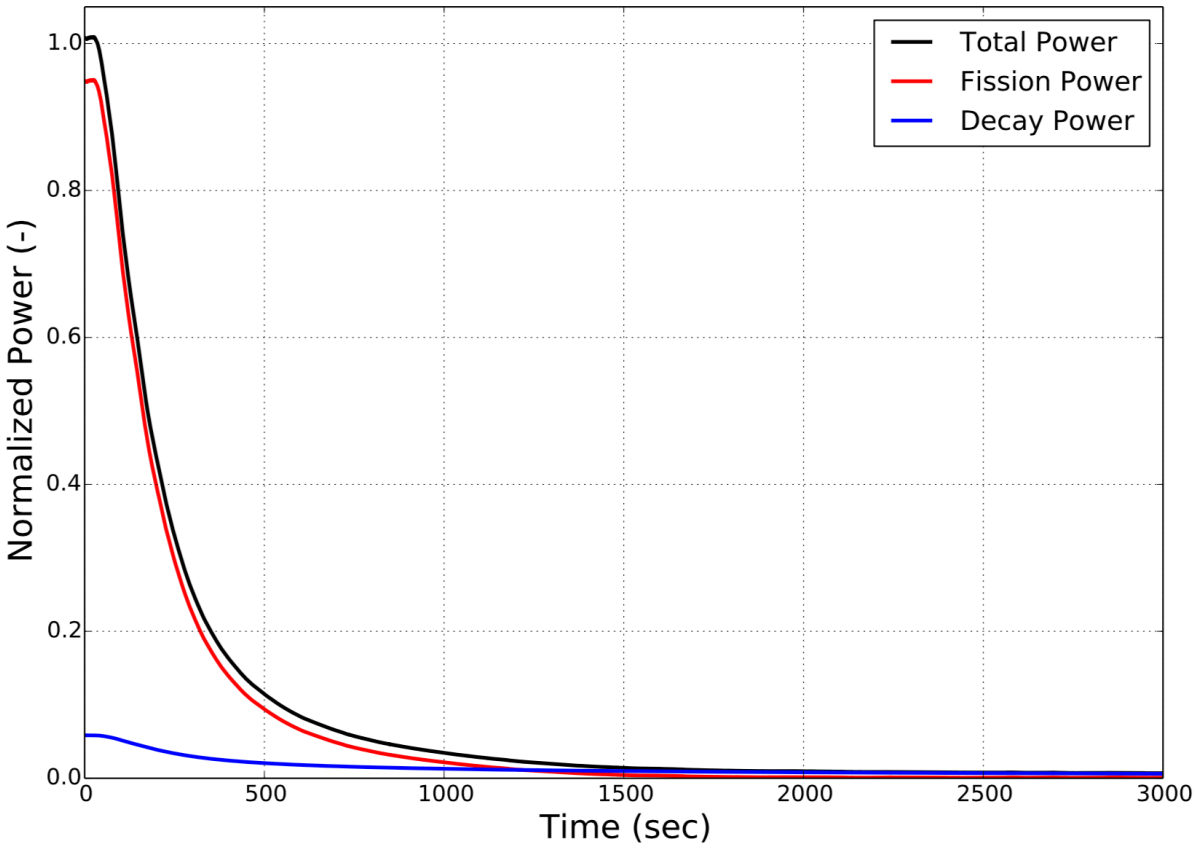

Figure 3.6. BOP-302R Normalized Power

A variety of thermocouples were installed to measure the core inlet and outlet temperatures. Figure 3.7 illustrates the high- and low-pressure inlet plena temperatures. Figure 3.8 illustrates the temperature of sodium at the Z-Pipe inlet. As for BOP-301, temperatures were also recorded at various elevations directly above a blanket subassembly within the outlet plenum but are not included in this report, since SAS4A/SASSYS-1 models the outlet plenum as a 0-dimensional volume and therefore cannot simulate a temperature distribution in the outlet plenum for comparison against these measured temperatures.

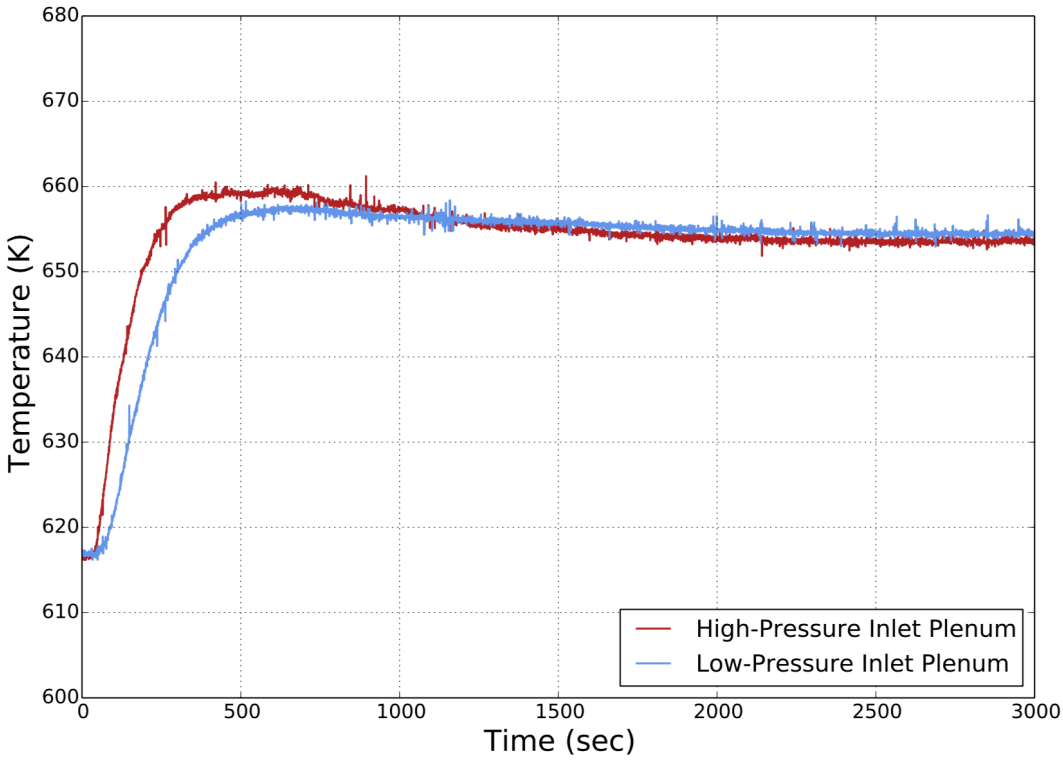

Figure 3.7. BOP-302R Core Inlet Temperature Measurements

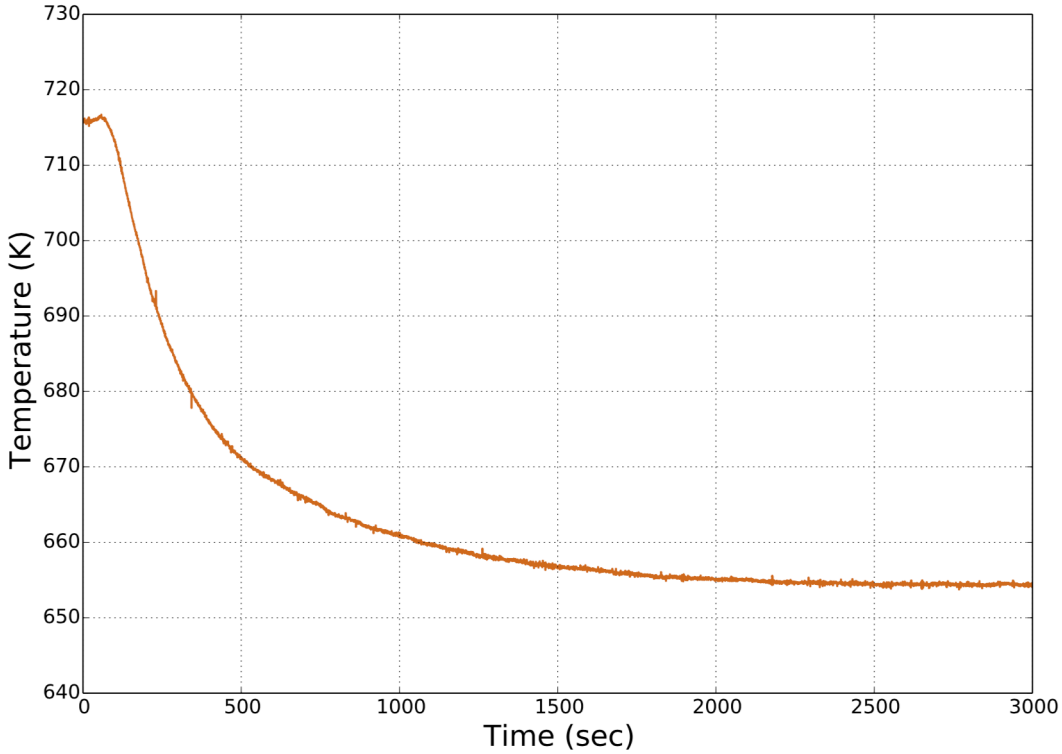

Figure 3.8. BOP-302R Z-Pipe Inlet Temperature Measurement

IHX primary-side temperatures are illustrated in Figure 3.9, but as with BOP-301, caution should be used when comparing the results of systems codes against these measurements. Again, the temperatures recorded by the outlet thermocouples were not representative of the average IHX outlet temperature. Temperatures measured at the bottom orifice plate, which was inside the IHX approximately one foot above the outlet, were significantly different from the measured outlet temperatures and were much more similar to the inlet temperature measurements following the decrease of heat rejection through the IHX.

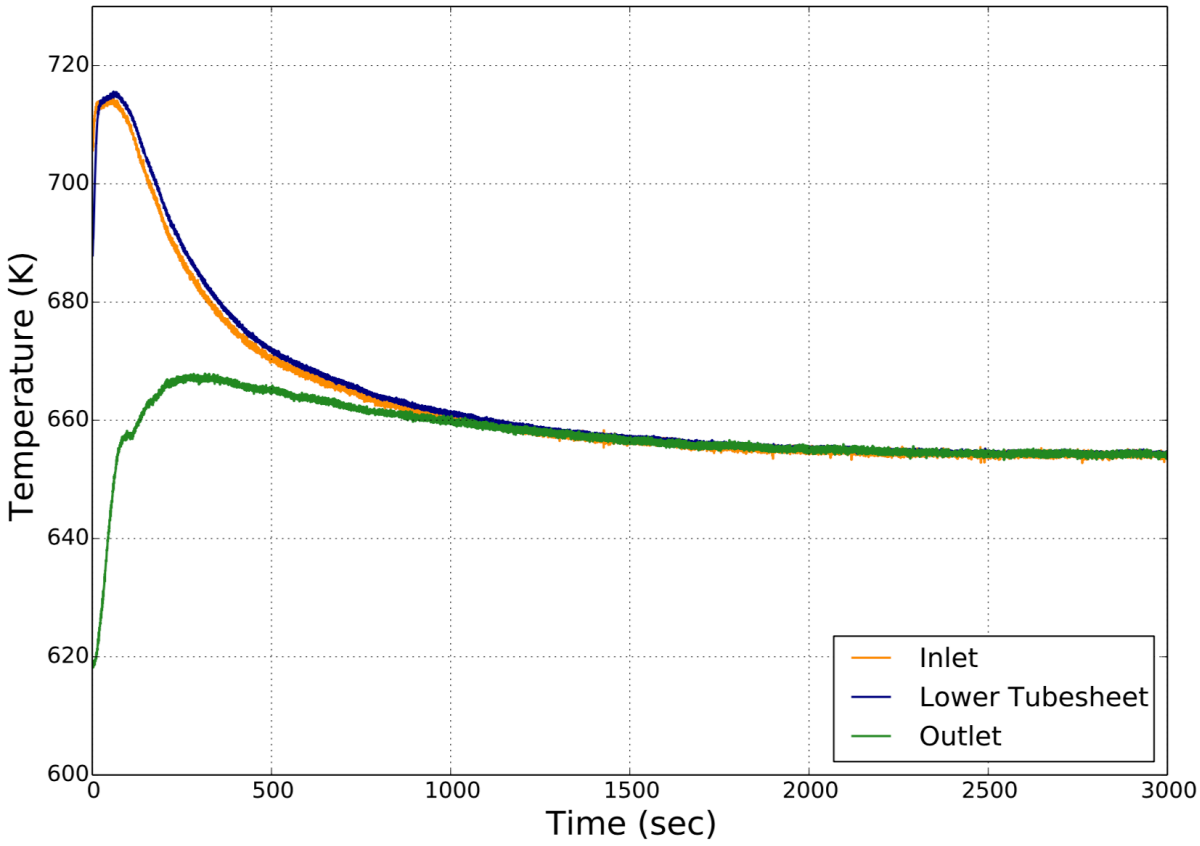

Figure 3.9. BOP-302R IHX Primary-Side Temperature Measurements

As for BOP-301, temperature changes throughout the primary system during BOP-302R produced small flow rate changes. Figure 3.10 illustrates the flow rates that were measured in the high- and low-pressure piping following Pump #2. Although ten flowmeters were originally installed in the primary system, the flowmeters in the piping following Pump #1 had failed prior to the SHRT testing program.

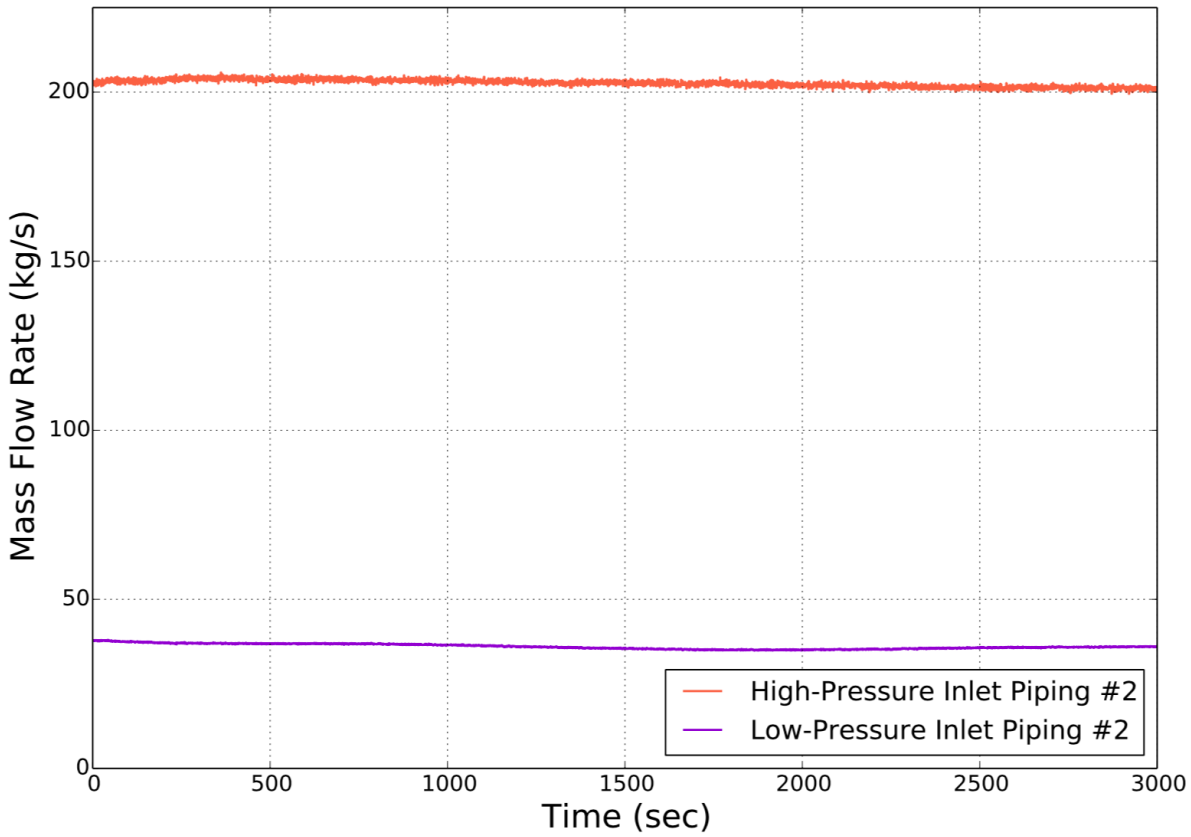

Figure 3.10. BOP-302R Primary Flow Measurements

4 SAS4A/SASSYS-1 Model

Argonne used the fast reactor safety analysis code SAS4A/SASSYS-1 for analysis of the SHRT and BOP tests. SAS4A/SASSYS-1 core models consist of a number of single-pin channels and optional subchannels. The single-pin channel model provides input to specify a single fuel pin and its associated coolant and structure. A single-pin channel represents the average pin in a subassembly, and subassemblies with similar reactor physics and thermal-hydraulic characteristics are grouped together and represented by a single channel.

Figure 4.1 illustrates the geometry used in the SAS4A/SASSYS-1 channel thermal-hydraulic model. SAS4A/SASSYS-1 models include axial zones to represent the fueled and gas plenum regions as well as up to six upper and lower reflector zones. Each axial zone is also connected to a structure region that can be used to model components such as the wire-wrap or duct walls.

At each axial location, temperatures are calculated at multiple radial nodes in the fuel, cladding, reflectors, and structure. A single bulk coolant temperature is assumed at each axial location. One-dimensional, radial heat transport calculations are performed at each axial segment from the fuel, through the cladding and into the coolant. Heat transfer is also calculated from the coolant to the gas plenum, reflector, and structure regions. The momentum equation is solved to determine the axial coolant flow. Convective heat transfer is assumed to dominate, so axial heat conduction is neglected.

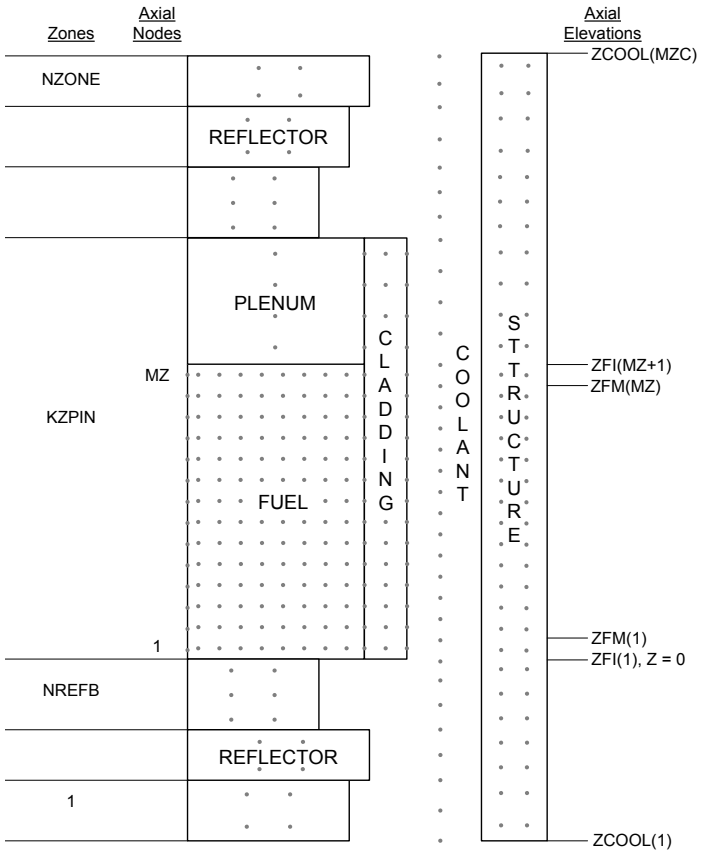

Figure 4.1. SAS4A/SASSYS-1 Core Channel Geometry

Analyses of the BOP-301 and BOP-302R tests were performed using a core model with 22 single-pin channels representing the 637 core subassemblies. Figure 4.2 illustrates how the 637 subassemblies were assigned to these 22 channels for these tests. The last two channels include the XX09 and XX10 instrumented subassemblies. The subassemblies surrounding XX09 and XX10 were included in Channels 21 and 22 for subchannel analysis that was performed for SHRT-17 and SHRT-45R for predicted detailed temperature distributions in the subassemblies. Subchannel analyses was not performed for the BOP tests.

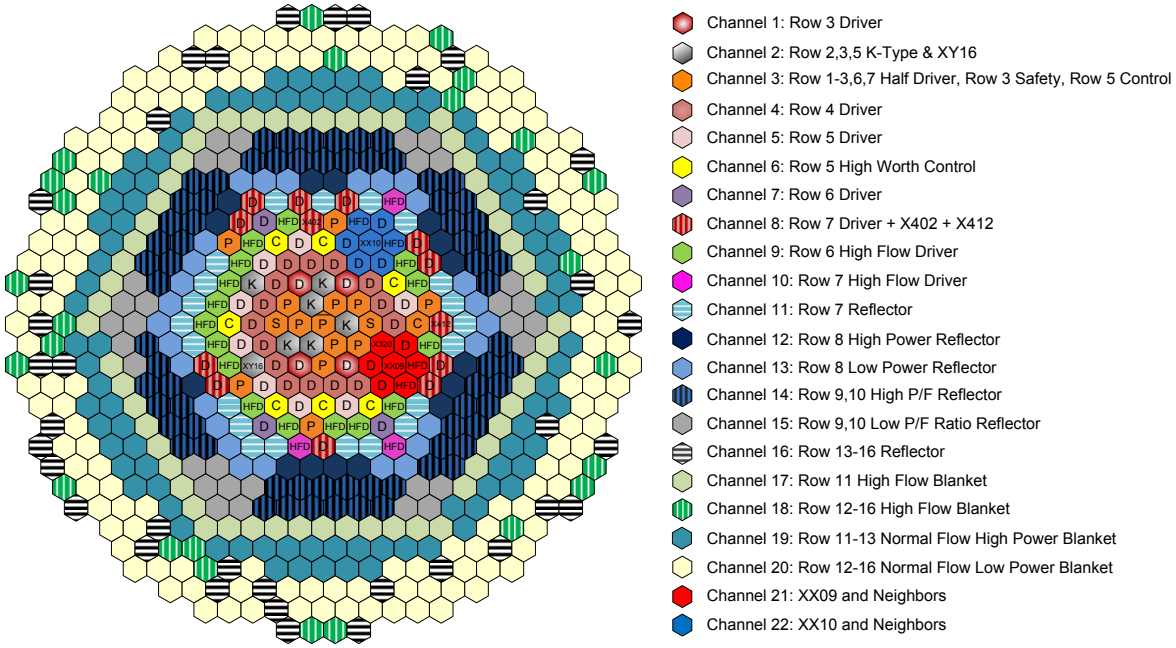

Figure 4.2. BOP-301 and BOP-302R SAS4A/SASSYS-1 Channels

The PRIMAR-4 module simulates the thermal hydraulics of the heat transport systems outside the core. In a PRIMAR-4 model, compressible volumes, or CVs, are zero-dimensional volumes that are used to model larger volumes of coolant such as inlet and outlet plena and pools. CVs are characterized by the pressure, temperature, elevation, and volume. Compressible volumes are connected by liquid segments, which are composed of one or more elements. Elements are modeled by one-dimensional, incompressible, single-phase flow and can be used to model pipes, valves, heat exchangers, steam generators, and more. Elements are characterized by their pressure, temperature, elevation, and mass flow rate.

Figure 4.3 illustrates the PRIMAR-4 model of the EBR-II primary sodium system. Sodium exits the high-pressure inlet plenum, CV1, and flows into Segment 1, representing the inner core subassemblies in Rows 1-7. The low-pressure inlet plenum, CV2, feeds Segment 2, which represents the outer core, reflector, and blanket subassemblies in Rows 8-16. Both segments discharge into the outlet plenum, CV3. Most of the sodium exits the outlet plenum through the Z-Pipe, which is represented by Elements 4-8 in Segment 4. Element 7 represents the auxiliary EM pump, which provides a small head during the BOP tests. Element 9 represents the primary side of the intermediate heat exchanger (IHX) and Element 10 represents the IHX outlet. Sodium leaving the IHX flows into the upper cold pool, CV4.

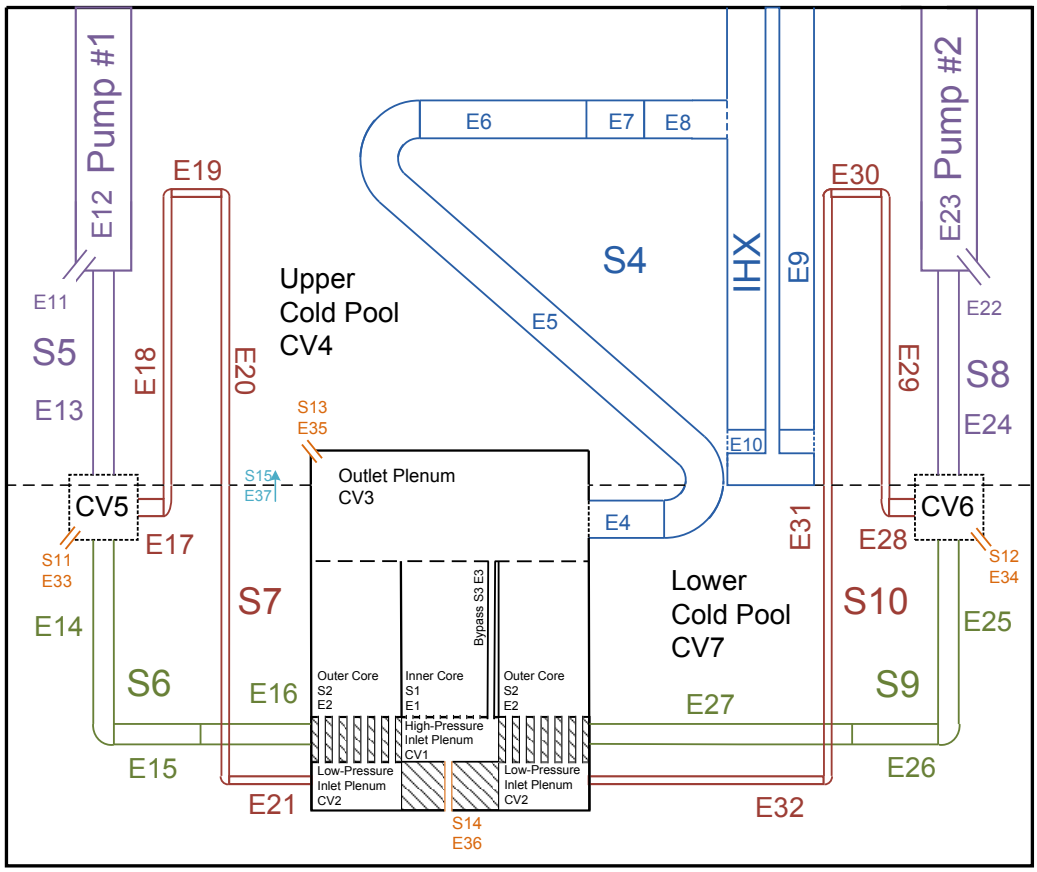

Figure 4.3. EBR-II Primary System PRIMAR-4 Model

During initial analyses of EBR-II, a single compressible volume was used to represent the entire cold pool. Recent model updates included splitting the cold pool into two volumes, with sodium below the IHX representing the cold, mostly stagnant sodium in the bottom part of the cold pool. Flow between the upper and lower cold pool volumes was set to 11.09 kg/s, which is equivalent to the leakage flow rates through Segments 11, 12, and 14.

Because the primary pumps remained on during the BOP tests, more mixing occurred in the cold pool during these transients than during SHRT-17 or SHRT-45R. Because of the size of the cold pool and the low flow rate between the two cold pool CVs, it is a slow process for the cold pool to come to equilibrium. For tests in which the primary pumps remain on, the pump inlet temperature could be accurately predicted by the upper cold pool temperature during the early portion of the test. As the tests continued, however, the influence of sodium mixing could not be accounted for by the relatively isolated upper and lower cold pools.

The component-to-component heat transfer model was used to represent mixing of the upper cold pool and the more stagnant lower cold pool through heat transfer. This model is based on a stagnant volume flow mixing model developed for the SAM code, which is discussed in greater detail in Reference 6. That model calculates the heat transfer rate between two volumes of different temperature where one volume is stagnant or nearly stagnant. The model can be represented in a simplified form as

$$Q = \dot{m}\, c_p\, \Delta T$$

where $\dot{m}$ is an assumed mixing flow rate, c_p is the sodium heat capacity, and ΔT is the temperature difference between the two pools.

The component-to-component heat transfer model represents heat transfer between the two volumes as

$$Q = h\, A\, \Delta T$$

where h is the heat transfer coefficient and A is the heat transfer surface area, both of which are assumed to be constant. By assuming that $\dot{m}$ and c_p are also constant, $h \times A$ can be set to $\dot{m} \times c_p$ to achieve a similar effect as the stagnant volume flow mixing model.

The upper cold pool volume is connected to two sets of core inlet piping represented by Segments 5-7 and 8-10. Except for small differences in the pump models, the two inlet piping sets are identical. Segments 5 and 8 represent the two primary sodium pumps, which draw sodium from the upper cold pool, and their inlets and outlets. CVs 5 and 6 are used to split the sodium discharged from the pumps into the high- and low-pressure inlet pipes. Segments 6 and 9 represent the two high-pressure inlet pipes and flow into the high-pressure inlet plenum. Segments 7 and 10 represent the two low-pressure inlet pipes and flow into the low-pressure inlet plenum.

Segments 11-14 represent the four leakage paths included in the model. Two different leakage flow paths are represented by Segment 13: leakage through the reactor cover and leakage at the IHX inlet. For the SAS4A/SASSYS-1 analysis, modeling these two leakages together has a negligible effect. In reality, however, a non-negligible amount of hot sodium may leak through either path at low flow rates, causing the IHX inlet temperatures to be lower than expected.

In addition to the stagnant volume flow mixing model, which was not necessary for the SHRT-17 and SHRT-45R models, the control system module was used in the simulations of the BOP tests to account for expansion of the portion of the control rod driveline in the cold pool. This simple model predicts the changing length of the control rod drivelines based on the temperature of the upper cold pool volume. Analysis of SHRT-45R did not use this model because the average cold pool temperature did not change more than a few degrees during that test.

5 Initial SAS4A/SASSYS-1 Predictions

In the following sections, the SAS4A/SASSYS-1 predictions of the BOP-301 and BOP-302R tests are compared against the measured test data. The predictions generally agree well with the measurements. For both tests, the biggest difference was that the predicted core inlet temperatures rose more quickly than the measured core inlet temperatures, which affected the rate of the fission power decrease at the beginning of the tests.

5.1 BOP-301

The BOP-301 test was initiated when the intermediate sodium pump tripped. The sodium flow rate in the intermediate loop decreased below 10% within 45 seconds, which led to a rapid reduction in the heat rejection rate through the IHX. Hotter sodium leaving the IHX on the primary side caused the cold pool temperature to increase. As this hot sodium flowed through the pump discharge piping, the core inlet temperature began to increase as well.

Figure 5.1 illustrates the measured and predicted high- and low-pressure inlet plena temperatures. The temperatures predicted by SAS4A/SASSYS-1 rise sooner than the measured temperatures because the cold pool is modeled with two 0-D volumes. As soon as hot sodium exits the IHX, the average temperature of the upper cold pool volume quickly rises. But in reality, there was some delay before sodium leaving the IHX reached the pump inlets, and this delay cannot be captured with simple 0-D volumes.

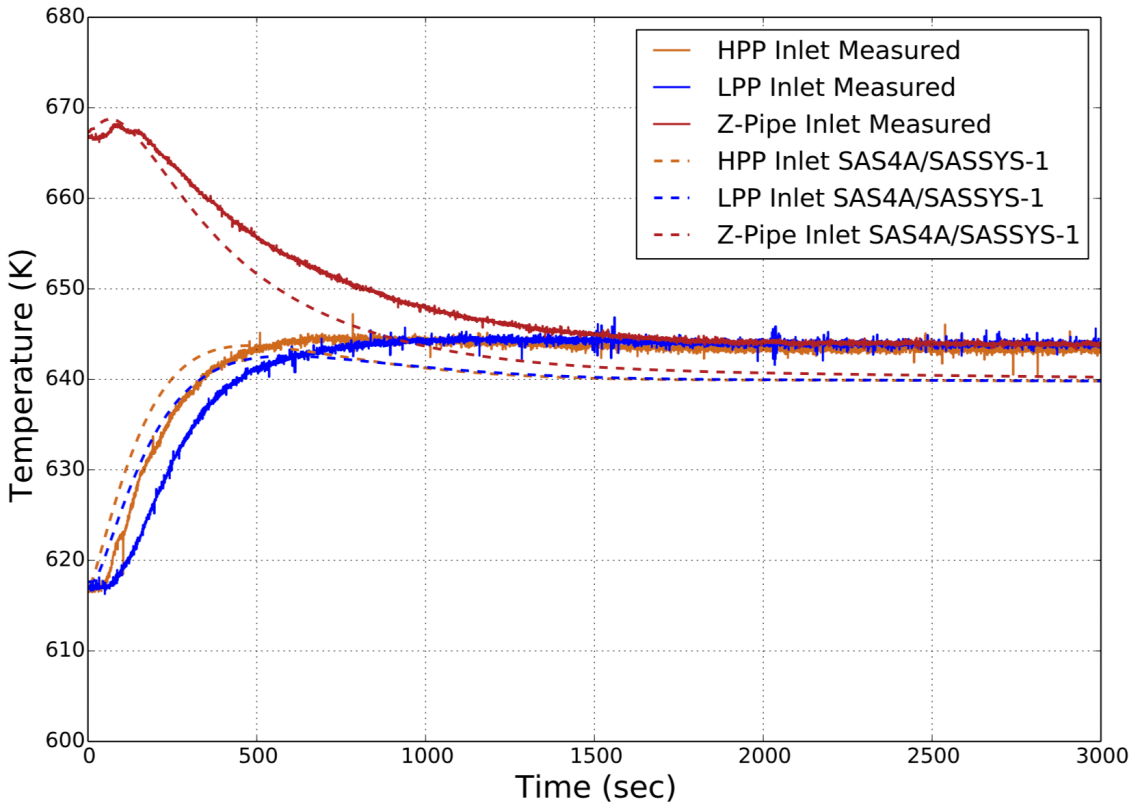

Figure 5.1. BOP-301 Core and Z-Pipe Inlet Temperatures

Reactivity feedbacks predicted by the SAS4A/SASSYS-1 model during BOP-301 are shown in shown in Figure 5.2. During a loss of heat sink transient, radial core expansion is typically the most negative reactivity feedback. Because the core inlet temperature increase lags behind the cold pool temperature, the reactivity feedback due to control rod driveline (CRDL) expansion is the largest initial source of negative reactivity, reaching negative 2.3¢ six minutes after the start of the test. The sodium density feedback also provides a sudden negative reactivity feedback as the core inlet temperatures begin to increase, reaching a minimum at negative 1.3¢.

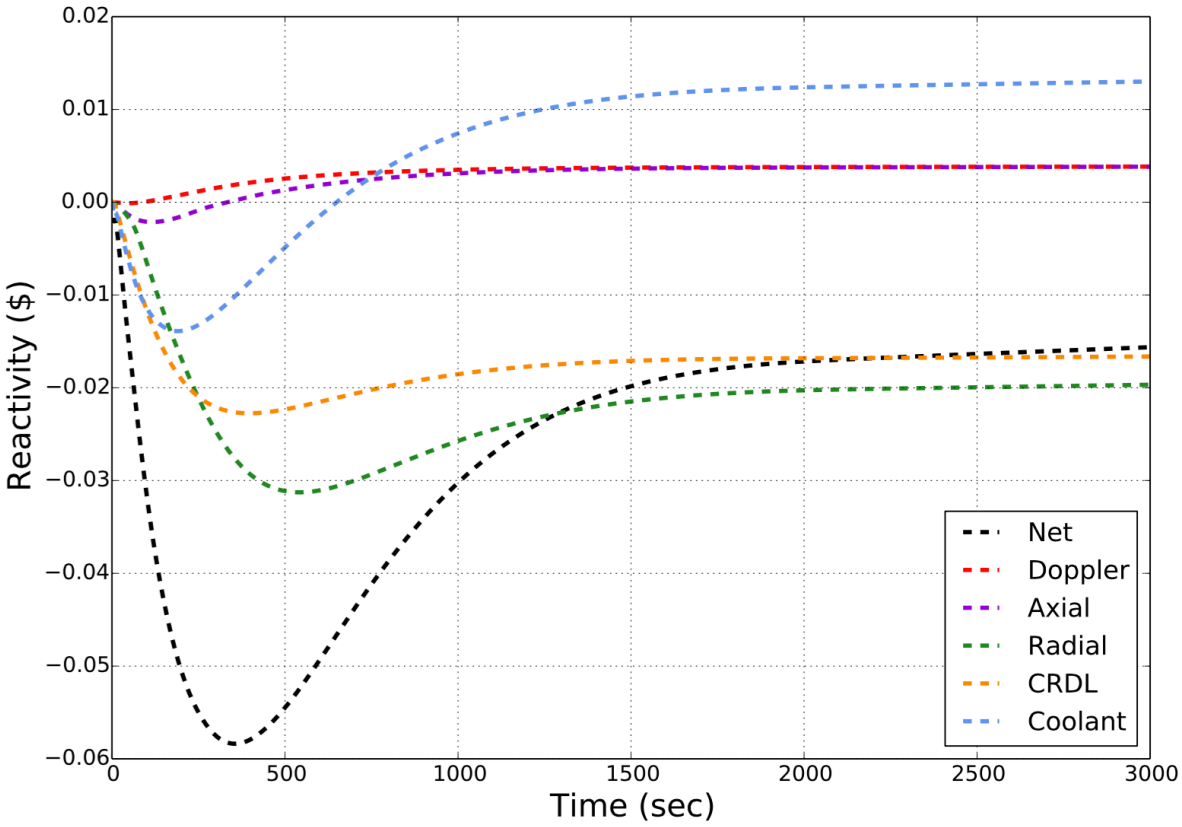

Figure 5.2. BOP-301 Reactivity Feedbacks

As power decreases, sodium temperatures at the top of the core begin to decrease. Neutron leakage is reduced and the sodium density feedback gets less negative and eventually becomes positive. The temperature of the control rod drivelines in the outlet plenum also decreases, which reduces the magnitude of the CRDL feedback. Meanwhile, the temperature of the grid plate catches up with the core inlet temperature, producing a negative radial core expansion feedback. The radial core expansion feedback surpasses the CRDL feedback and generates enough negative reactivity to compensate for the increasing and soon-to-be positive sodium density feedback. The Doppler and axial expansion feedbacks are not strong contributors to the BOP-301 transient.

Figure 5.3 illustrates the measured and predicted total power level during BOP-301. Because the cold pool is modeled with two 0-D volumes, the control rod driveline and core

inlet temperatures increase faster in the simulation than they likely did during the actual test. This leads to a faster insertion of negative reactivity from those two feedbacks, causing the predicted power level to decrease faster than the measured power. While the core inlet temperature is overpredicted during the first 500 seconds of the transient, the predicted total power level continues to decrease faster. By 1500 seconds, temperatures throughout the system have stabilized. Decay heat represents nearly half of the total power production by this time, and both the measured and predicted total power have leveled off below 2% of the nominal power level.

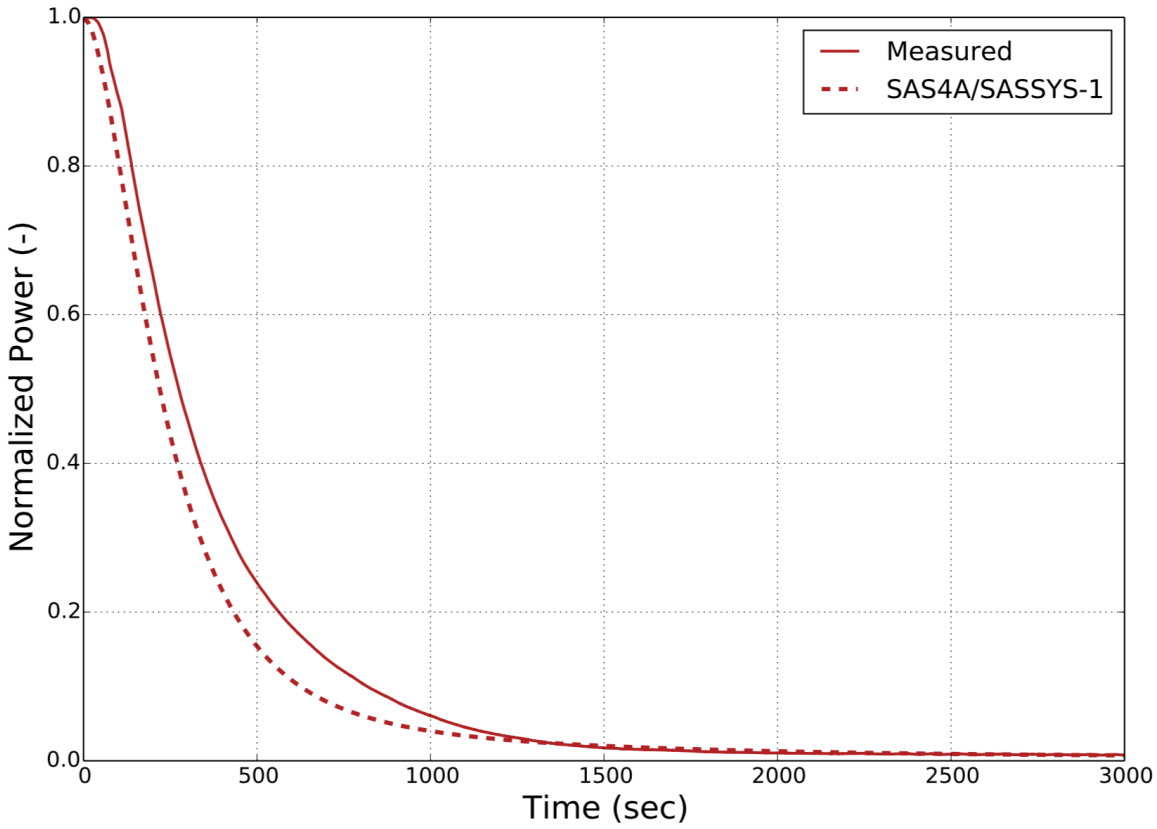

Figure 5.3. BOP-301 Total Power

Figure 5.1 above also illustrates the measured and predicted Z-Pipe inlet temperature. The predicted Z-Pipe inlet temperature decreases more quickly due to the faster drop in the predicted total power. With total power decreasing below 2% and full primary sodium flow maintained, the temperature rise across the core becomes very small. The core outlet and Z-Pipe inlet temperatures converge to the core inlet temperature.

Ultimately, the predicted temperatures throughout the primary system converge at 640 K, within 5 K of the actual test measurements. Additional comparisons for the IHX temperatures are not provided in this report, as there are concerns about whether or not those measurements reflect average sodium temperatures at those locations. These concerns were discussed in Section 3.

5.2 BOP-302R

Like BOP-301, the BOP-302R test was initiated when the intermediate sodium pump tripped. With less heat rejection through the IHX, the IHX primary-side outlet temperature began to increase. As temperatures throughout the cold pool increased, the core inlet temperature began to rise, inducing negative reactivity feedbacks to drive down the total power level.

Figure 5.4 illustrates the measured and predicted high- and low-pressure inlet plena temperatures. After the intermediate pumps trip, the IHX primary side outlet temperature increases nearly to the core outlet temperature. Because the temperature rise across the core is nearly twice as large for BOP-302R, there is a larger difference between the IHX primary-side outlet and cold pool temperatures after heat rejection through the IHX is lost. Consequently, the cold pool heats up faster for BOP-302R. The difference between the measured and predicted temperatures was smaller for BOP-302R than for BOP-301, especially for the high-pressure inlet plenum. The predicted low-pressure inlet plenum temperature still rises faster than the measured data, but the difference is not as much as for BOP-301.

As temperatures throughout the primary system converge, the predicted core inlet and Z-Pipe inlet temperatures agree well with the measured data. The difference between the predicted and measured temperatures is less than 5 K at the end of the test. The predicted primary system temperatures converge a little later than the measured temperatures because the SAS4A/SASSYS-1 model predicts a slightly larger power level at the end of the test.

The BOP-302R model predicted that the system converged to a temperature approximately 5 K higher than the measured data. Conversely, the BOP-301 model predicted that the system converged to a lower temperature than the measured data. The reason for this difference is not clear, but it was postulated that not capturing subassembly bowing with the simple radial expansion model might be the primary reason for this difference. For these tests, a slightly higher or lower temperature may be required to provide the necessary reactivity feedback from the radial core expansion model to return the system to a net reactivity of zero following the core inlet temperature increase.

Figure 5.5 illustrates the reactivity feedbacks during BOP-302R, which are similar to BOP-301, except larger in magnitude. The CRDL reactivity feedback still provides the most negative reactivity during the first few minutes of the test as the cold pool temperature increases. As with BOP-301, the sudden decrease in the core inlet temperature produces a fast negative sodium density reactivity feedback. But temperatures at the top of the core decrease more than the temperatures at the bottom of the core increase, so the sodium density feedback reaches a minimum after only 100 seconds, before increasing and becoming positive.

Seven minutes into the test, the radial expansion feedback becomes the most negative feedback before reaching a minimum at negative 4.2¢. Temperatures in the top half of the core decrease even more than for BOP-301, limiting the magnitude of the feedback effect, which levels off around negative 2.9¢. The Doppler and axial expansion reactivity feedbacks are very small for this test as well and do not exceed 1.0¢.

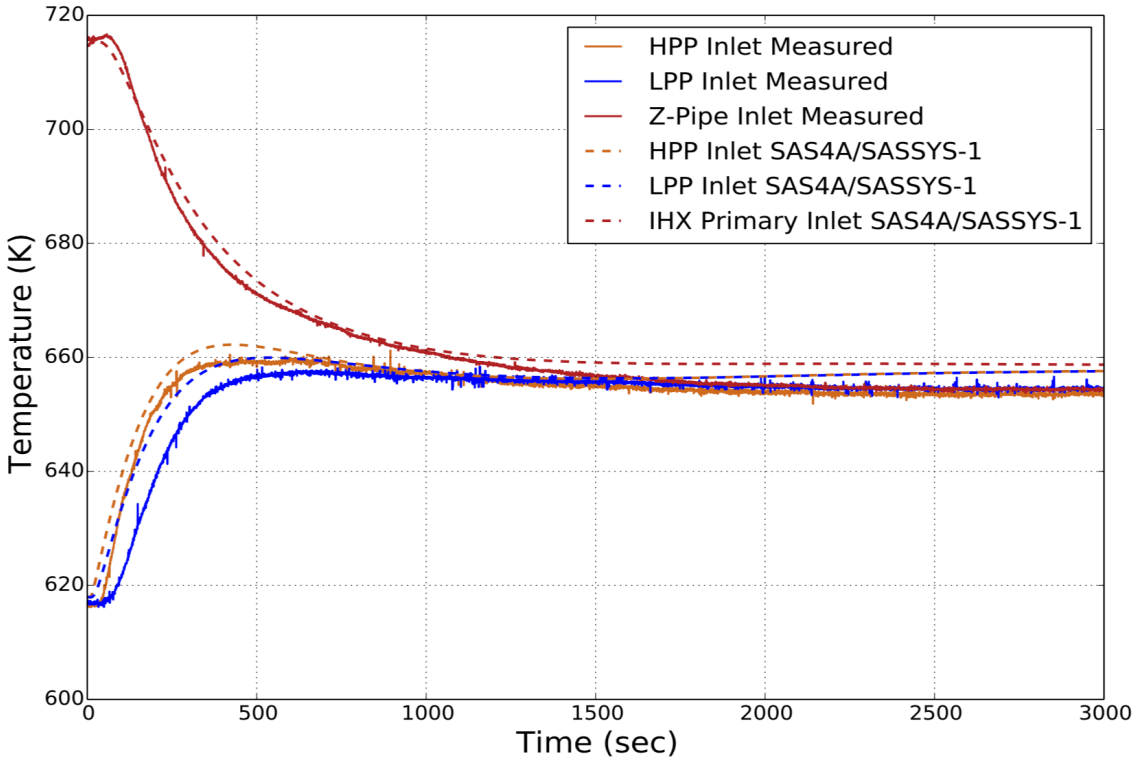

Figure 5.4. BOP-302R Core and Z-Pipe Inlet Temperatures

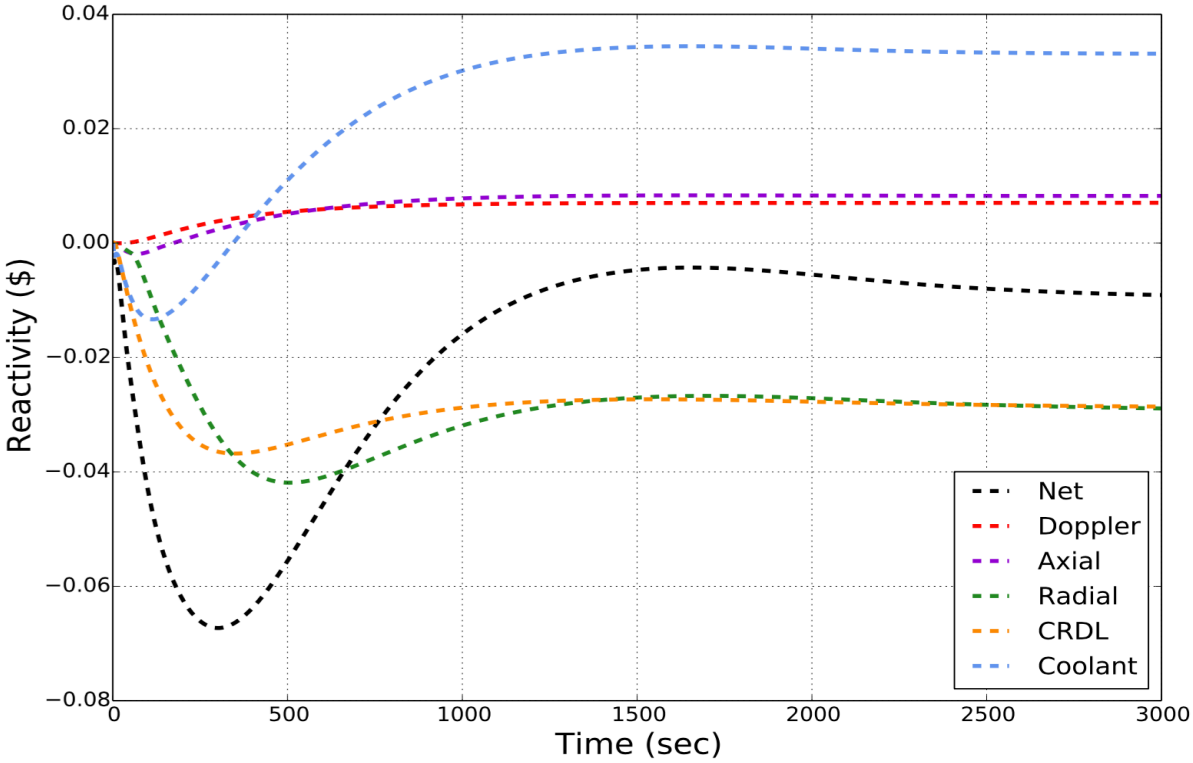

Figure 5.5. BOP-302R Reactivity Feedbacks

Figure 5.6 illustrates the BOP-302R measured and predicted total power levels, which agree much better than for BOP-301. The improved agreement is partially due to better agreement for the high-pressure inlet plenum temperature. However, the radial core expansion reactivity feedback model also has a significant impact on these results. SAS4A/SASSYS-1 does not have a model accurately representing EBR-II's freestanding core with spacer buttons that are intended to prevent inward subassembly bowing. Instead, SAS4A/SASSYS-1's simple radial expansion model was used, which predicts the average expansion of the core based on temperature changes at the core inlet and an elevation corresponding to the above-core load pads. This model was used with the input parameters adjusted to predict the expansion at the location of the middle spacer button.

Beyond using a very simple radial core expansion model, the model is also very sensitive to the temperatures of these two tests. For both BOP-301 and BOP-302R, the core inlet temperature rises and the core outlet temperature decreases, resulting in a small temperature change at the core midplane. Because of the way the simple radial expansion model input parameters were defined, the predicted radial expansion feedback strongly follows the core midplane temperature. Small differences in the core midplane temperature, therefore, have a relatively large effect on the radial expansion feedback, which is the most negative reactivity feedback effect. The negative radial expansion feedback may have been overpredicted with the simple model for BOP-301, leading to a faster power decrease, and well predicted for BOP-302R, leading to better agreement with the measured total power.

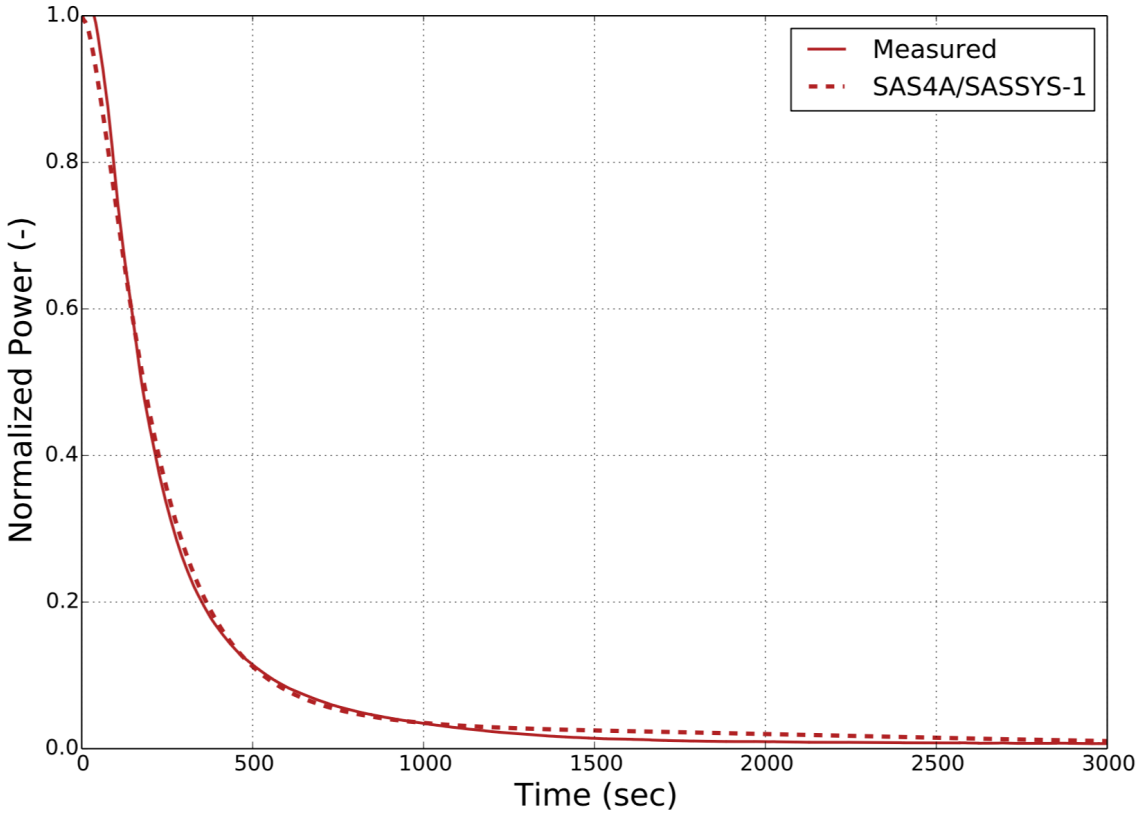

Figure 5.6. BOP-302R Total Power

6 Uncertainty Quantification and Optimization

Advancements in the knowledge of nuclear reactor performance have led to an increased need to perform Sensitivity Analyses (SA) and Uncertainty Quantification (UQ) in the advanced reactor domain. The role of uncertainty quantification spans many facets in the nuclear industry, including system design and optimization, licensing, and probabilistic risk assessment [7].

SAS4A/SASSYS-1 has been recently coupled with Dakota via a Python interface to extend the capabilities of the Argonne safety code for uncertainty quantification and design optimization. The Dakota software [8], which is maintained by Sandia National Laboratory, is an uncertainty quantification and optimization toolkit that has been in development for over 20 years. With the new coupling package, Dakota samples user specified parameters, performs SAS4A/SASSYS-1 transient simulations with those parameters, and completes post processing by quantifying statistical metrics. Dakota is also capable of performing calibration in order to resolve discrepancies between the simulation results and the experimental data.

Several key parameters from the BOP-301 and BOP-302R SAS4A/SASSYS-1 inputs were selected for evaluation with Dakota based on engineering judgment. This analysis is intended to evaluate the impact that reactivity feedback coefficients, cold pool parameters, and other inputs have on the agreement between simulation predictions and measured test data. Following the sensitivity analyses, the uncertain parameters found to have relatively large impacts were optimized by Dakota to assess the magnitude of changes needed to improve the agreement between the simulation results and the measured data.

6.1 Dakota and SAS4A/SASSYS-1 Coupling

A Python interface was developed to couple Dakota with SAS4A/SASSYS-1. The Dakota executable is available pre-compiled via the Sandia National Laboratory website [8], and coupling with SAS4A/SASSYS-1 is accomplished via a black-box interface. Data communication between Dakota and SAS4A/SASSYS-1 occurs through parameter and response files. Uncertain parameters in the SAS4A/SASSYS-1 input template are replaced with random values generated by Dakota. Then, SAS4A/SASSYS-1 simulations are initiated, and the response values of interest from the simulations are saved for processing by Dakota. Figure 6.1 illustrates this coupling scheme.

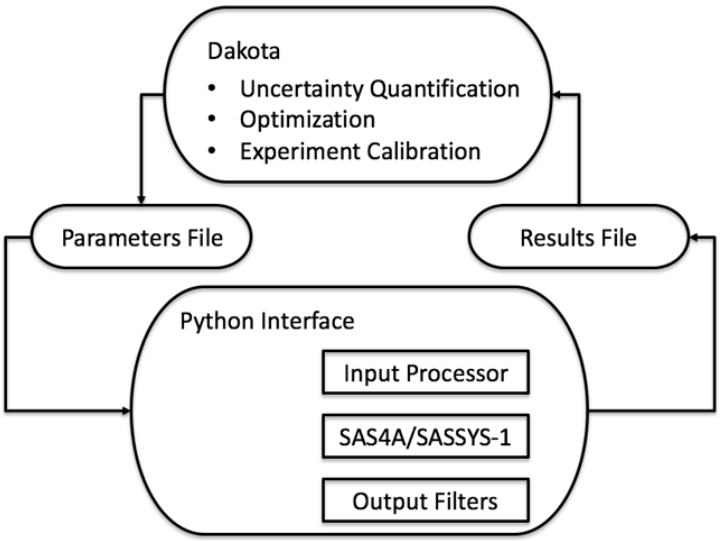

Figure 6.1. Dakota and SAS4A/SASSYS-1 Coupling Scheme

A Dakota input file is composed of the methodology, variables, interface, and responses for the uncertainty quantification and design optimization process. A series of sampling-based techniques is implemented in Dakota for uncertainty propagation. The Monte Carlo method is one of the most popular sampling techniques and involves random sampling with specific distributions on the uncertain domain.

Another sampling-based technique for uncertainty propagation, Latin Hypercube Sampling (LHS), was used for the uncertainty quantification of the BOP-301 and BOP-302R simulations. Latin Hypercube Sampling, which is illustrated in Figure 6.2 is a method for exploring the input space of an uncertain domain divided into N segments. The relative length of each segment is determined by the probability distribution. Every subgroup in each of the uncertain variables is randomly assigned to a sample only one time. There is no restriction on the number of bins, but LHS requires all uncertain variables to have the same number of bins. The total number of samples equals the number of bins. LHS is expected to require fewer samples than traditional Monte Carlo method to achieve the same statistical accuracy [8].

The responses of interest are written in a result file and returned to Dakota for the quantification of the statistical metrics. Means, standard deviations, and 95% confidence intervals are computed for each of the responses. In addition, Dakota calculates the most common statistics between uncertainties and responses of interest including the covariance, Pearson coefficient, and other correlations. The Pearson coefficient is a measure of the linear correlation between two variables, and its value ranges between +1 to -1, inclusive. A Pearson coefficient with a large absolute value means that two variables are strongly correlated. A positive Pearson coefficient represents a positive correlation while a negative value indicates that the two variables are inversely correlated.

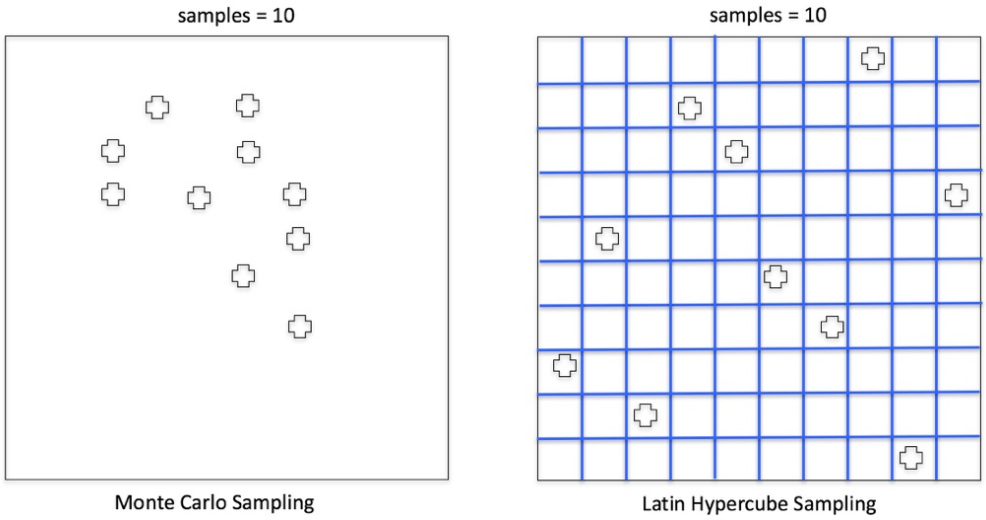

Figure 6.2. Examples of Monte Carlo and Latin Hypercube Sampling Techniques

6.2 Sensitivity Analysis of the EBR-II BOP Simulation

Fourteen input parameters were considered for the sensitivity analysis of the BOP-301 and BOP-302R simulations. Those parameters, including the

- RDEXPC: Radial core expansion reactivity feedback worth coefficient,
- XMCXAC: Radial core expansion reactivity feedback geometry parameter,
- ADOP: Flooded Doppler coefficient,
- FUELRA: Fuel reactivity worth per unit mass,
- CLADRA: Cladding reactivity worth per unit mass,
- VOIDRA: Coolant void worth per unit mass,
- CRDEXP: Control rod driveline thermal expansion coefficient,
- ACRDEX and BCRDEX: Control rod driveline expansion reactivity feedback coefficients,
- RDTUHX: Product of density and specific heat for the IHX tubes,
- G2PRDR: Intermediate loop orifice coefficient,
- DTMPTB: Transient steam generator sodium outlet temperature,
- FLOSSL: Initial total core mass flow rate,
- VOLLGC: Volume of sodium in the lower cold pool CV, and
- HAELHT: Heat transfer coefficient for the cold pool flow mixing model.

The first eight parameters were included to evaluate the sensitivity of the transient predictions to the reactivity feedback models in the code. The spatially-dependent reactivity feedback coefficients for fuel, cladding, coolant voiding, and the Doppler effect were treated as correlated parameters such that each coefficient for a single feedback effect was perturbed

by the same fraction. The variables were assumed to be uniformly distributed within the ranges determined by engineering judgement.

The EBR-II SAS4A/SASSYS-1 input utilizes the simple radial core expansion reactivity feedback model. It assumes that grid plate expansion is proportional to either the core inlet sodium temperature or the temperature of the walls in the inlet plenum, and that expansion of the duct walls is proportional to the average temperature change of the structure at the elevation of the load pads. While EBR-II did not have load pads, each subassembly had pressed dimple-type spacer buttons on the outside of the subassembly near the core midplane. These spacer buttons were intended to prevent core compaction. The simple radial core expansion model is represented by

$$\Delta\rho_{radial} = C_{radial}[\Delta T_{inlet} + \frac{XMC}{XAC}(\Delta\bar{T}_{load\ pads} - \Delta T_{inlet}]$$

where

$\Delta\rho_{radial}$ = reactivity feedback due to radial core expansion, \$

C_{radial} = radial core expansion reactivity feedback coefficient, \$/K

ΔT_{inlet} = core inlet temperature change, K

XMC = distance from the grid plate to the core midplane, m

XAC = distance from the grid plate to the above core load pads, m

$\Delta\bar{T}_{load\ pads}$ = average structure temperature change at the load pad elevation, K.

The ratio of XMC to XAC allows the model to approximate the expansion at the core midplane based on ΔT_{inlet} and $\Delta\bar{T}_{load\ pads}$. This ratio was defined to account for the expansion at the location of the spacer buttons near the core midplane.

The next three parameters after the reactivity feedback parameters are included to evaluate the impact of the intermediate loop on the transient results. The first intermediate loop parameter, the product of density and specific heat for the IHX tubes, affects the predicted heat transfer rate through the IHX. If the IHX tubes are represented as being thicker than the specification indicates, lower initial intermediate sodium temperatures will be predicted to achieve the necessary heat rejection from primary sodium to secondary sodium through the IHX.

The second intermediate loop parameter is one of the loss coefficients in the intermediate loop. This loss coefficient is an artificially large user-specified value in the input to ensure there is sufficient hydraulic resistance in the intermediate loop to achieve the specified intermediate loop flow rates. Intermediate loop geometry was not provided in the benchmark so a simple representative loop was used to achieve the specified mass flow rate boundary condition. The large loss coefficient produces a larger pressure drop than any buoyancy forces in the intermediate loop. Consequently, the specified mass flow rate can be achieved through a user-specified table of pump head vs. time without influence from buoyancy during the transient.

The final intermediate loop parameter is the steam generator sodium outlet temperature during the transient. During the steady-state calculation, SAS4A/SASSYS-1 calculates the

necessary IHX intermediate-side inlet temperature based on user-specified flow rates and geometry as well as the primary-side inlet and outlet temperatures. The steam generator outlet temperature is set equal to the IHX inlet temperature during steady-state. But during the transient, the steam-generator outlet temperature can be defined by a user-specified table. This table was used to achieve the IHX intermediate-side inlet temperature boundary condition specified in the benchmark. Changing the transient steam generator outlet temperature allows for evaluating the sensitivity of the simulation predictions to the IHX intermediate-side inlet temperature boundary condition.

The initial core mass flow rate was included in the sensitivity analysis to investigate the impact of uncertainties in the specified initial conditions for each test.

The final two parameters considered for the sensitivity analysis are related to the flow mixing model used for the cold pool. The first parameter is the amount of the total cold pool that is represented by the lower cold pool CV. The remainder of the cold pool is treated with the upper cold pool. The other parameter determines the mixing between the two cold pool CVs represented by the flow mixing model. This parameter is the product of heat transfer coefficient times heat transfer area, which, as discussed in Section 4, represents the product of mass flow rate between the two volumes and sodium heat capacity.

Four test measurements were used to evaluate how changes to the parameters listed above affect test predictions:

- Z-pipe inlet temperature,
- High-pressure inlet plenum (HPP) temperature,
- Low-pressure inlet plenum (LPP) temperature, and
- Normalized power.

Since the experimental data and the SAS4A/SASSYS-1 simulation results were at different time intervals, the SAS4A/SASSYS-1 simulation results were processed by piecewise linear interpolation. Then, the root mean square (RMS) between the simulation results and experimental data was calculated as a measure of the agreement. Therefore, a lower RMS value means that the SAS4A/SASSYS-1 simulation results are closer to the measurements.

The Latin Hypercube Sampling technique was applied for the uncertainty propagation, and the fourteen uncertain parameters were perturbed simultaneously. The user-specified perturbation ranges are listed in Table 6.1 along with the results of the sensitivity analysis. The Pearson coefficient between the perturbed uncertainty and the RMS value is an indicator of the agreement between the benchmark results and the measured data. Since the fourteen variables are investigated simultaneously, it is computationally expensive to converge the results. Instead, each of the uncertainties is assigned a score based on a binned approach such that two uncertainties exhibit similar impacts if the calculated Pearson coefficients fall within the same bin range. Table 6.1 divides the resulting Pearson Coefficients into three categories:

- "+" indicating that the measured and predicted data get closer by perturbing the variable (|Pearson Coefficient| > 0.05),
- "++" for |Pearson Coefficient| > 0.1, indicating an even more significant improvement, (|Pearson Coefficient| > 0.10) and
- "N/A" indicating the perturbation of the uncertain variable has a minimal impact on the simulation results. (|Pearson Coefficient| < 0.05).

Table 6.1. Impact of Uncertain Variables on SAS4A/SASSYS-1 Predictions

	Nominal Value	**Range (Uniform Distribution)**	**$T_{z\text{-pipe inlet}}$**	**$T_{HPP\text{-inlet}}$**	**$T_{LPP\text{-inlet}}$**	**Power**
Radial expansion feedback coefficient ($/K)	-0.00266	±20%	++	++	++	+
XMC/XAC ratio	0.96546	0.0001 - 0.9999	++	++	++	++
Flooded Doppler coefficient (Δk/k)	space dependent	±20%	N/A	N/A	N/A	N/A
Fuel expansion coefficient (Δk/k-kg)	space dependent	±20%	N/A	N/A	N/A	N/A
Cladding expansion coefficient (Δk/k-kg)	space dependent	±20%	N/A	N/A	N/A	N/A
Coolant reactivity coefficient (Δk/k-kg)	space dependent	±20%	N/A	N/A	N/A	N/A
Control rod drive thermal expansion coefficient (1/K)	2.0×10^{-5}	±30%	++	+	+	+
Control rod expansion feedback coefficient ($/m)	-15.61	±20%	+	+	+	N/A
Heat exchange coefficient between upper and lower sodium volumes (W/K)	298609	0.1 - 400000	++	++	++	N/A
Lower sodium pool volume (m^3)	186.576	40 - 260	++	++	++	++
Steam generator outlet temperature (K)	548	±10	N/A	N/A	N/A	N/A
Resistance in the intermediate loop	4000000	0.0 - 5000000.0	N/A	N/A	N/A	N/A
Initial primary flow rate (kg/s)	468.7	±5%	++	+	+	N/A
Density*specific heat of tube in IHX (J/m^3-K)	4.36×10^{6}	±10%	N/A	N/A	N/A	N/A

During the BOP-301 and BOP-302R simulations, radial core expansion contributes the most negative reactivity feedback. Control rod driveline expansion also provides a large amount of negative reactivity. Unsurprisingly, the parameters related to these two effects have a significant impact on the benchmark results. On the contrary, axial expansion and the Doppler effect produce relatively small reactivity feedbacks during these tests, and therefore their impact is very limited.

Since the primary pumps remained on during the BOP tests, significant sodium mixing occurred between the upper and lower sodium volumes, and the corresponding parameters (i.e. the lower sodium pool volume and pool mixing heat transfer coefficient) strongly affect the simulation results. Perturbations of the initial primary flow rate affect the core outlet and Z-Pipe inlet temperatures. The results are therefore very sensitive to initial flow rate perturbations. Perturbations to the steam generator outlet temperature and the flow resistance of the intermediate loop both have a negligible impact on the agreement between test measurements and simulations predictions. The sensitivity analysis also demonstrated that the product of density and specific heat for the IHX tubes has a negligible impact on the benchmark results.

6.3 Optimization of EBR-II BOP Simulation Results

The sensitivity analysis demonstrated that the radial expansion reactivity feedback, control rod drive expansion reactivity feedback, and cold pool flow pool mixing models have the largest impacts on the benchmark results. Following the sensitivity analysis, the Dakota-SAS4A/SASSYS-1 toolkit was used to identify the optimal values for those input parameters to improve the agreement between measured test data and simulation predictions.

The hybrid optimization method implemented in Dakota was used to find global optima for perturbations of the following the input variables:

- Radial expansion reactivity feedback coefficient,
- XMC/XAC ratio,
- Heat transfer coefficient between upper and lower cold pool CVs,
- Volume of sodium in the lower cold pool CV,
- Control rod driveline thermal expansion coefficient, and
- Initial primary mass flow rate.

For most of these parameters, the optimization process searched for a single parameter to use for both tests. BOP-301 and BOP-302R were performed during the same testing window and had the same core load configuration. Therefore, the optimized cases should have the same reactivity feedback coefficients. Additionally, considering the large volume of the sodium pool and the fact that the flow rates in the two cases are close, the same cold pool flow mixing model should be applied to both cases.

For two parameters, the optimization process searched for different values for BOP-301 and BOP-302R. Those parameters were the XMC/XAC ratio and the initial primary mass flow rate. BOP-302R was initiated at a higher power level than BOP-301. Different structure temperatures result in a different distribution of forces on the space buttons throughout the

core. For one test, expansion may be best approximated by temperatures at the core midplane, while for another, lower temperature changes could result in the core inlet temperature being most appropriate for the simple radial expansion model. And different initial mass flow rates were searched for the two cases in order to accommodate the uncertainty of the primary flow rate measurements, which were used as initial boundary conditions.

The Dakota-SAS4A/SASSYS-1 coupling is capable of evaluating the objective responses from a multi-model study. In each sample, Dakota updated the BOP-301 and BOP-302R SAS4A/SASSYS-1 input files with random values within user-specified ranges and the simulations were conducted independently. Four responses of interest in each BOP case were sent back to Dakota for post-processing:

- Z-Pipe inlet temperature
- HPP inlet temperature
- LPP inlet temperature
- Normalized power

Root mean square values were calculated between the simulation results and the experimental measurements. Dakota used the optimization mode to minimize these RMS values. It initialized 350 samples on the whole uncertain domain shown in Table 6.1 and the global optimum was narrowed down to a small region. Then, Dakota continued the local search until the uncertain parameters converged, resulting in the optimized parameters provided in Table 6.2. Figures 6.3-6.6 illustrate that the agreement between the SAS4A/SASSYS-1 predictions and the measurements is greatly improved.

For the radial core expansion reactivity feedback coefficient, control rod driveline thermal expansion coefficient, and initial core flow rate the differences between the original and optimized parameters are small. The optimized XMC/XAC ratio for BOP-301 is also relatively unchanged from the initial value. For BOP-302R, the optimized XMC/XAC ratio is decreased significantly. This indicates that grid plate expansion becomes increasingly important for loss of heat sink transients as the temperature rise across the core increases. Perhaps the lower power level of BOP-301, the core is less compact and able to expand freely at the level of the spacer buttons. But at full power for BOP-302R, there is less core flowering and radial expansion is driven by the grid plate primarily.

Different values for the cold pool flow mixing model were also found during the optimization process. Approximations were used for the original values for the heat transfer coefficient and lower cold pool sodium volume. Further investigation will be necessary in the future to better understand the proper values to use for these parameters during various transient scenarios.

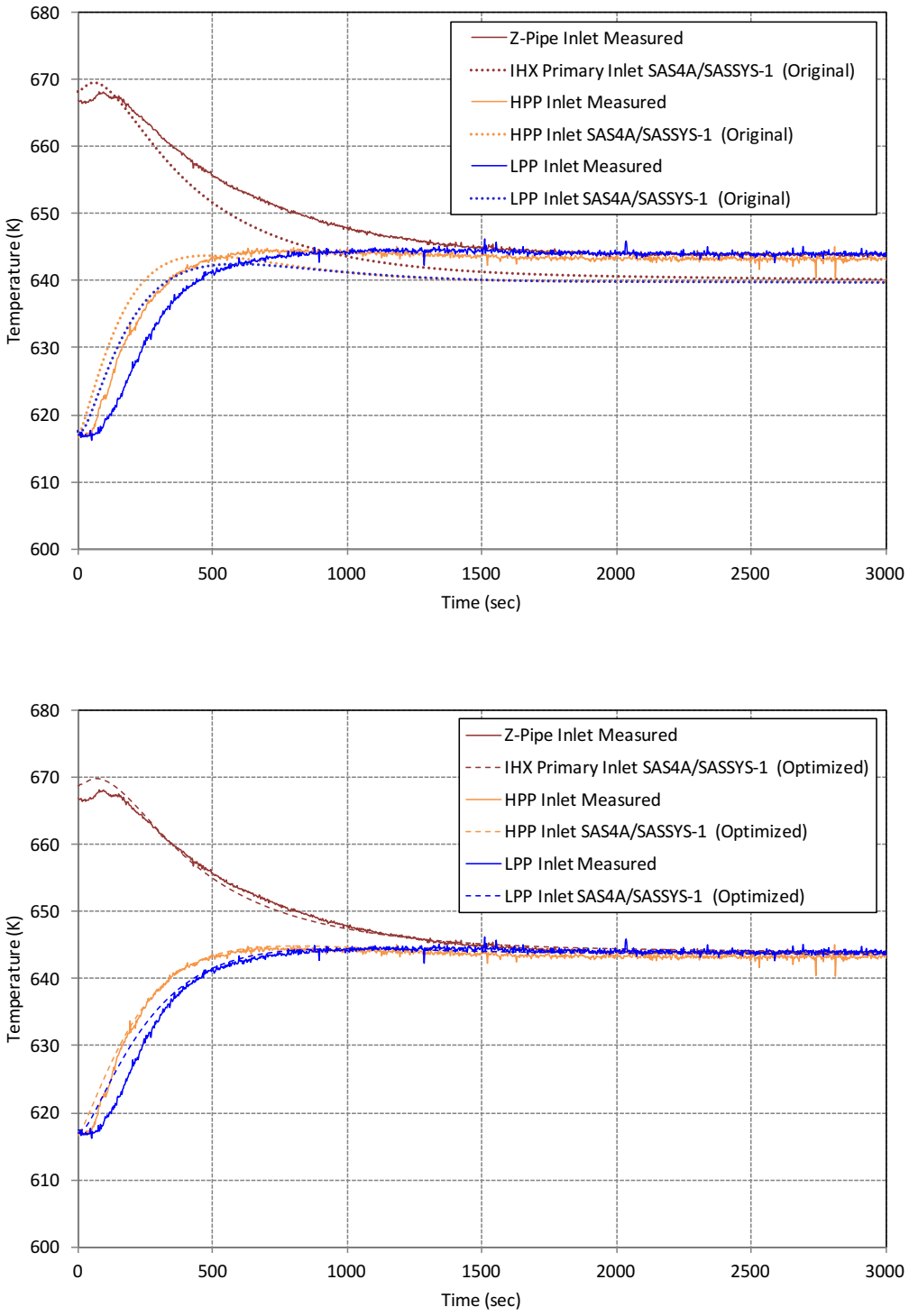

Figure 6.3. BOP-301 Core Inlet and Z-Pipe Inlet Temperatures – Original (Upper) vs. Optimized (Lower) models

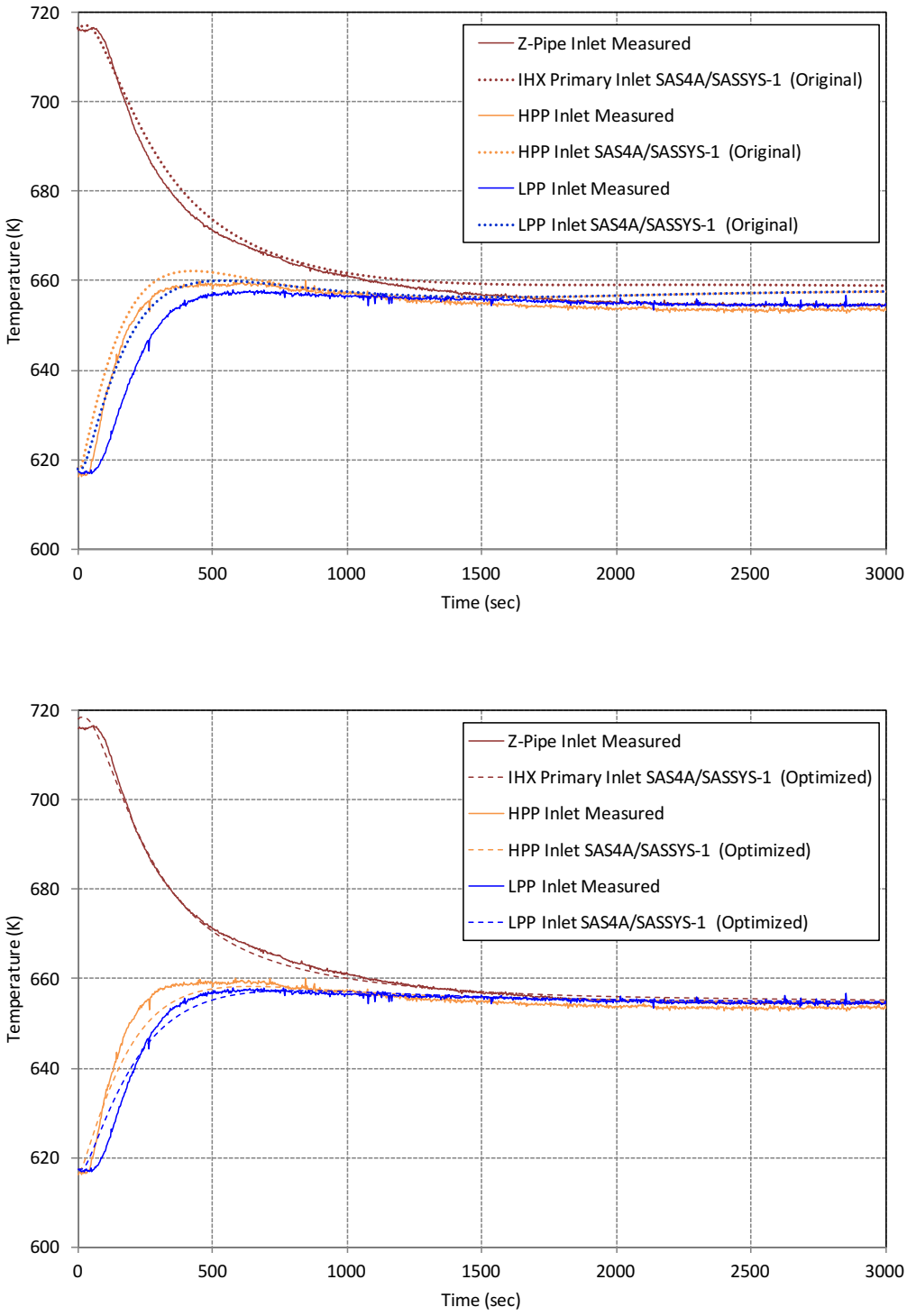

Figure 6.4. BOP-302R Core Inlet and Z-Pipe Inlet Temperatures – Original (Upper) vs. Optimized (Lower) models

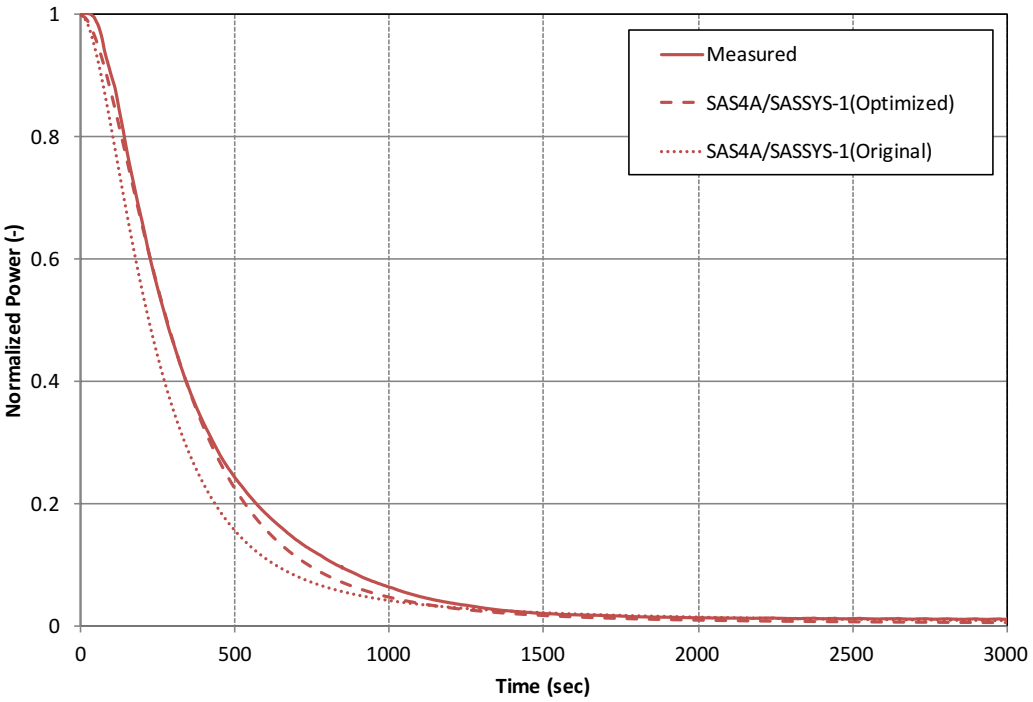

Figure 6.5. BOP-301 Total Power

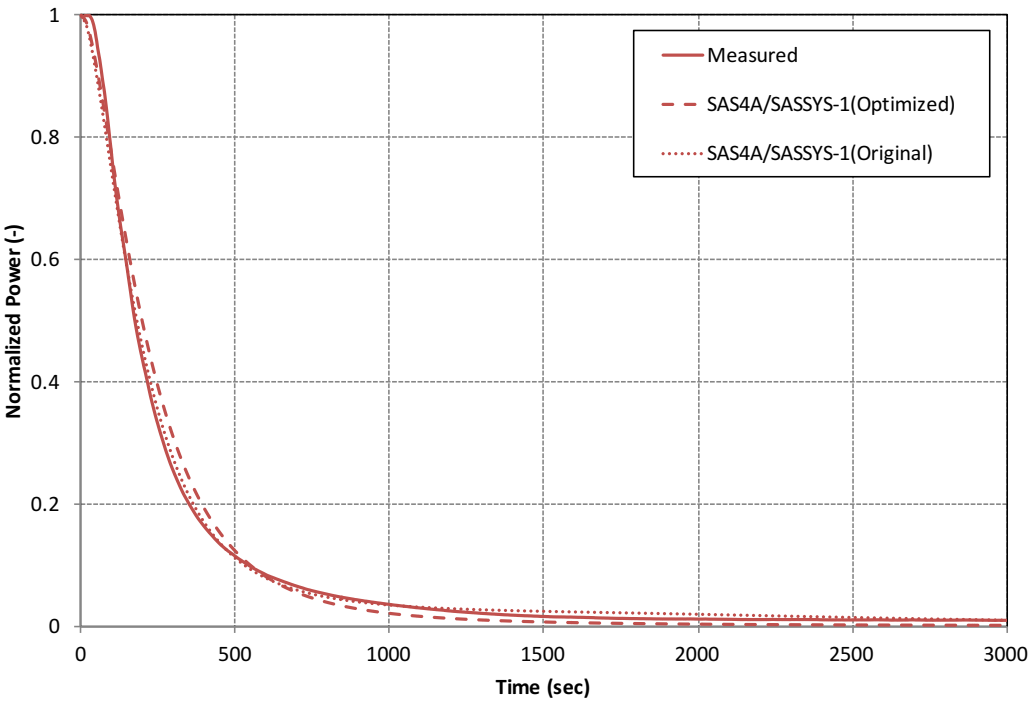

Figure 6.6. BOP-302R Total Power

Table 6.2. Optimized SAS4A/SASSYS-1 Inputs Parameters

	Reference	**BOP-301 Optimized**	**BOP-302R Optimized**
Radial expansion feedback coefficient ($/K)	-0.00266	-0.00222	-0.00222
Initial primary flow rate (kg/s)	468.7 for BOP-301 466.9 for BOP-302R	463.6	458.1
XMC/XAC ratio	96.5%	99.8%	29.7%
Heat transfer coefficient between upper and lower sodium pool (W/K)	298609	202208	202208
Lower sodium pool volume (m^3)	186.6	109.9	109.9
Control rod drive thermal expansion coefficient (1/K)	2.00×10^{-5}	1.70×10^{-5}	1.70×10^{-5}

7 Summary

The BOP-301 and BOP-302R tests were performed during the same SHRT testing window as the landmark SHRT-45R test. Because of the low flow rate during SHRT-45R, uncertainty in the flow measurements was high. Argonne has continued its EBR-II analysis by simulating and analyzing BOP-301 and BOP-302R, two unprotected loss of heat of sink tests in which the intermediate sodium pump tripped without scramming the control rods or tripping the primary pumps. The BOP tests were selected for this analysis in order to assess the EBR-II SAS4A/SASSYS-1 model under different conditions while having higher confidence in the accuracy of the flow measurements.

Initial predictions from simulations of the BOP-301 and BOP-302R tests agreed well with the measured test data. The agreement for the BOP tests was similar to the agreement for the SHRT analysis performed for an IAEA coordinated research project. The core inlet temperature changed much more during the two BOP tests than during the two SHRT tests. By implementing a simple stagnant volume flow mixing model for the cold pool, reasonable agreement was obtained with the measured core inlet temperatures, especially the high-pressure inlet plenum temperature. The low-pressure inlet plenum temperature may be affected by heat transfer between the low-pressure inlet piping and the thermally stratified cold pool, which cannot be properly accounted for by the SAS4A/SASSYS-1 model.

Agreement with the measured total power level varied for SHRT-45R and the BOP tests. From the previous SHRT-45R analysis, power was slightly underpredicted during the beginning of the test and overpredicted at the end of the test. For BOP-301, the model predicted a faster decrease of the total power as the core inlet temperatures were predicted to increase faster than the measured temperatures. Although the power prediction was slightly higher for BOP-302R at the end of the test, the model for this test obtained the best agreement with the measured power. Use of the simple radial core expansion reactivity feedback model may have been responsible for agreement with the measured power level differing among the three tests. Without a radial core expansion model that better represents EBR-II's unique core restraint system, which has not been used in more recent fast reactor designs, capturing the behavior of radial core expansion during different scenarios with a single model may be difficult.

For SHRT-45R, the Z-Pipe inlet temperature was well predicted. Agreement with the measured Z-Pipe inlet temperature was even better for the BOP-301 and BOP-302R models. Z-Pipe outlet and IHX primary-side inlet temperatures were not discussed in this report. For both SHRT loss of flow tests, the SAS4A/SASSYS-1 predictions of the IHX inlet temperature did not agree with the measured data. It has been speculated that the location of the IHX inlet thermocouple, along with leakage at the IHX inlet and thermal stratification within the Z-Pipe, caused the poor agreement. Analysis of the BOP tests produced similarly poor agreement at the IHX inlet. CFD analysis along the Z-Pipe and at the IHX inlet may be required to properly understand how temperatures vary at the inlet of the IHX. However, despite the poor agreement with the measured IHX temperatures, agreement between the measured data and model predictions throughout the rest of the primary system was very good for the BOP-301 and BOP-302R tests.

The Dakota-SAS4A/SASSYS-1 package was applied to further evaluate discrepancies between SAS4A/SASSYS-1 simulation predictions and experimental data. Fourteen

uncertainties were simultaneously perturbed within user-specified ranges using the Latin Hypercube Sampling technique. Sensitivity analysis demonstrated that the radial core expansion, control rod driveline expansion, and cold pool flow mixing models had the largest impacts on the simulation results.

Following the uncertainty quantification, the input parameters identified to have large impacts on both BOP-301 and BOP-302R simulations were optimized by Dakota such that the SAS4A/SASSYS-1 simulation results are in even better agreement with the test measurements. The optimization changes are relatively modest. The recommended radial expansion coefficient is less negative but within the uncertain range from engineering judgment. The two optimized BOP simulations exhibit quite different radial core expansion behavior, likely due to the different initial power levels and thermal gradients. Optimized values were also found for the cold pool flow mixing model, which used assumed values for the initial simulations.

ELECTRONIC APPENDIX A

Electronic Appendix A is the Excel file BOP-301_Measured_Data_for_Comparison.xls.

ELECTRONIC APPENDIX B

Electronic Appendix B is the Excel file BOP-302R_Measured_Data_for_Comparison.xls.

References

1. Briggs, L. L., T. Sumner, T. Fei, T. Sofu, and S. Monti, "EBR-II Passive Safety Demonstration Tests Benchmark Analyses – Phase 1", *Trans. Amer. Nucl. Soc.*, Anaheim, California, USA, November 9-13, 2014, **111**, pp. 1263-1266.
2. Briggs, L., *et al.*, "EBR-II Passive Safety Demonstration Tests Benchmark Analyses – Phase 2", *Proc. of the 16th International Topical Meeting on Nuclear Reactor Thermal Hydraulics (NURETH-16)*, Chicago, Illinois, USA, August 30-September 4, 2015.
3. T. H. Fanning, A. J. Brunett, and T. Sumner, eds., *The SAS4A/SASSYS-1 Safety Analysis Code System*, ANL/NE-16/19, Nuclear Engineering Division, Argonne National Laboratory, March 31, 2017.
4. T. Sumner and T.Y.C. Wei, "Benchmark Specifications and Data Requirements for EBR-II Shutdown Heat Removal Tests SHRT-17 and SHRT-45R," ANL-ARC-226 (Rev 1), Argonne National Laboratory report, May 31, 2012.
5. T. Fei, A. Mohamed, and T. K. Kim, "Neutronics Benchmark Specifications for EBR-II Shutdown Heat Removal Test SHRT-45R – Revision 1," ANL-ARC-228 (Rev 1), Argonne National Laboratory report, January 23, 2013.
6. Hu, Rui, and T. Sumner, "Benchmark Simulations of the Thermal-Hydraulic Responses During EBR-II Inherent Safety Tests Using SAM", *ICAPP '16*, San Francisco, California, USA, April 17-20, 2016. Manuscript submitted for publication.
7. BRIGGS, L.L., "Uncertainty Quantification Approaches for Advanced Reactor Analyses", ANL-GenIV-110, Argonne, IL, September 30, 2008.
8. ADAMS, B.M., et. al., "Dakota, A Multilevel Parallel Object-Oriented Framework for Design Optimization, Parameter Estimation, Uncertainty Quantification, and Sensitivity Analysis: Version 6.0 User's Manual," Sandia Technical Report SAND2014-4633, July 2014. Updated November 2015 (Version 6.3).

Nuclear Science and Engineering Division
Argonne National Laboratory
9700 South Cass Avenue, Bldg. 208
Argonne, IL 60439-4842

www.anl.gov

Argonne National Laboratory is a U.S. Department of Energy
laboratory managed by UChicago Argonne, LLC